BOARD LEVEL RELIABILITY ASSESSMENT OF THICK FR-4 QFN ASSEMBLIES UNDER THERMAL CYCLING

by

TEJAS SHETTY

Presented to the Faculty of the Graduate School of

The University of Texas at Arlington in Partial Fulfillment

of the Requirements

for the Degree of

MASTER OF SCIENCE IN MECHANICAL ENGINEERING

THE UNIVERSITY OF TEXAS AT ARLINGTON

DECEMBER 2014

DEDICATION

This thesis is dedicated to my family. I also dedicate this thesis to my teachers from whom I have learnt so much.

ACKNOWLEDGEMENTS

I would like use this opportunity to express my gratitude to Dr. Dereje Agonafer for giving me a chance to work at EMNSPC and for his continuous guidance during that time. It has been a wonderful journey working with him in research projects and an experience to learn so much from the several conference visits. I also thank him for serving as the committee chairman.

I would like to thank Dr. A. Haji-Sheikh and Dr. Kent Lawrence for serving on my committee and providing numerous learning opportunities.

I would like to extend a special appreciation to Fahad Mirza, who was not only the PhD mentor but also a good friend who helped me throughout my thesis and academics. I want to thank all the people I met at EMNSPC and for their support during my time. Special thanks to Sally Thompson, Debi Barton, Catherine Gruebbel and Louella Carpenter for assisting me in almost everything. You all have been wonderful.

I would like to thank Alok Lohia and Marie Denison for their expert inputs while working on the SRC funded project, the result of which is part of this thesis.

I also would like to mention, without all my friends' constant annoyance, I would have completed my thesis much earlier.

November 17, 2014

ABSTRACT

BOARD LEVEL RELIABILITY ASSESSMENT OF THICK FR-4 QFN ASSEMBLIES UNDER THERMAL CYCLING

Tejas Shetty, M.S.

The University of Texas at Arlington, 2014

Supervising Professor: Dereje Agonafer

Quad Flat No-Lead (QFN) packages gained popularity in the industry during the last decade or so due to its superior thermal/electrical characteristics, low cost and compact size. QFN packages are widely used in handheld devices where space is a constraint; however, some customers require it for industry application demanding thicker printed circuit boards (PCB's). As the thickness of PCB increases, the fatigue life (MTTF) of the solder joints decreases. QFN being a leadless package, its board level thermo-mechanical reliability is a critical issue. This provides the motivation for this work. The QFN package on thick board was experimentally characterized under accelerated thermal cycling (ATC) loading. This test exhibited numerous insufficient joints and zero standoff height or a combination of both across the package edge. The primary objective of this work is to understand and mitigate the root cause of the solder joint failure and provide

guidelines to improve the fatigue life of the package. Design for reliability methodology was used to approach this problem. Initially a parametric three-dimensional (3D) finite element (FE) model for the QFN package on thick PCBs was formulated in ANSYS. The fatigue correlation parameter was determined by simulation and various energy based and strain based models are examined to predict the characteristic life (cycles to 63.2% failure). A methodology to derive a new power equation to accurately predict the fatigue life has been proposed. Furthermore, design analysis of QFN was performed to study the effects of several key package parameters on the solder joint reliability. The results from FE modeling and reliability testing will be leveraged to propose “best practices” to have a robust design.

TABLE OF CONTENTS

LIST OF ILLUSTRATIONS

LIST OF TABLES

Chapter 1

INTRODUCTION AND OBJECTIVE

1.1 Role of Packaging in Micro-Electronics

The semiconductor industry has witnessed the continuous development of new and enhanced processes leading to highly integrated and reliable circuits. One such process is complementary metal oxide semiconductor (CMOS) process which is being extensively used for the manufacture of Integrated Circuits (IC's) [1].

An IC consists of substrate and layers of thin films with their thicknesses ranging from approximately 100 nm to 1μm. For a typical CMOS process these films include:

- Semiconductors (as active part)
- Metal interconnects
- Via plugs (as carrier for current),
- Dielectrics (for electrical isolation),
- Passivation layers (for mechanical protection).

The substrate in an IC acts like mechanical carrier during processing. Figure 1.1 shows a cross-section of a typical IC.

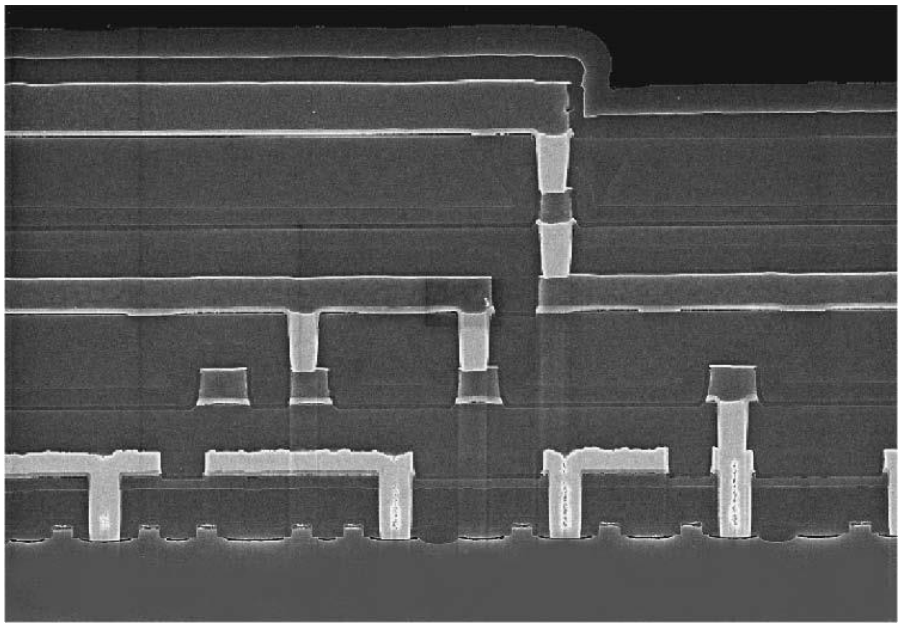

Figure 1.1 Cross section of a typical IC

After IC manufacturing in the waferfab, the next process in the assembly is the packaging. Packaging plays a vital role in any electronic device from the performance and cost standpoint. It is the whole package that is shipped and not just the silicon; packaging significantly contributes to the total cost - equal to or greater than that of the silicon. The primary functions of a package are:

- Allow an IC to be handled for PC Board assembly
- Mechanical and chemical protection against the environment
- Enhance thermal and electrical properties
- Allow standardization (footprints)

Packages can be broadly classified as (see Figure 1.2):

- Through Hole Mount IC Packages
- Surface Mount IC Packages
- Contactless Mount IC Packages

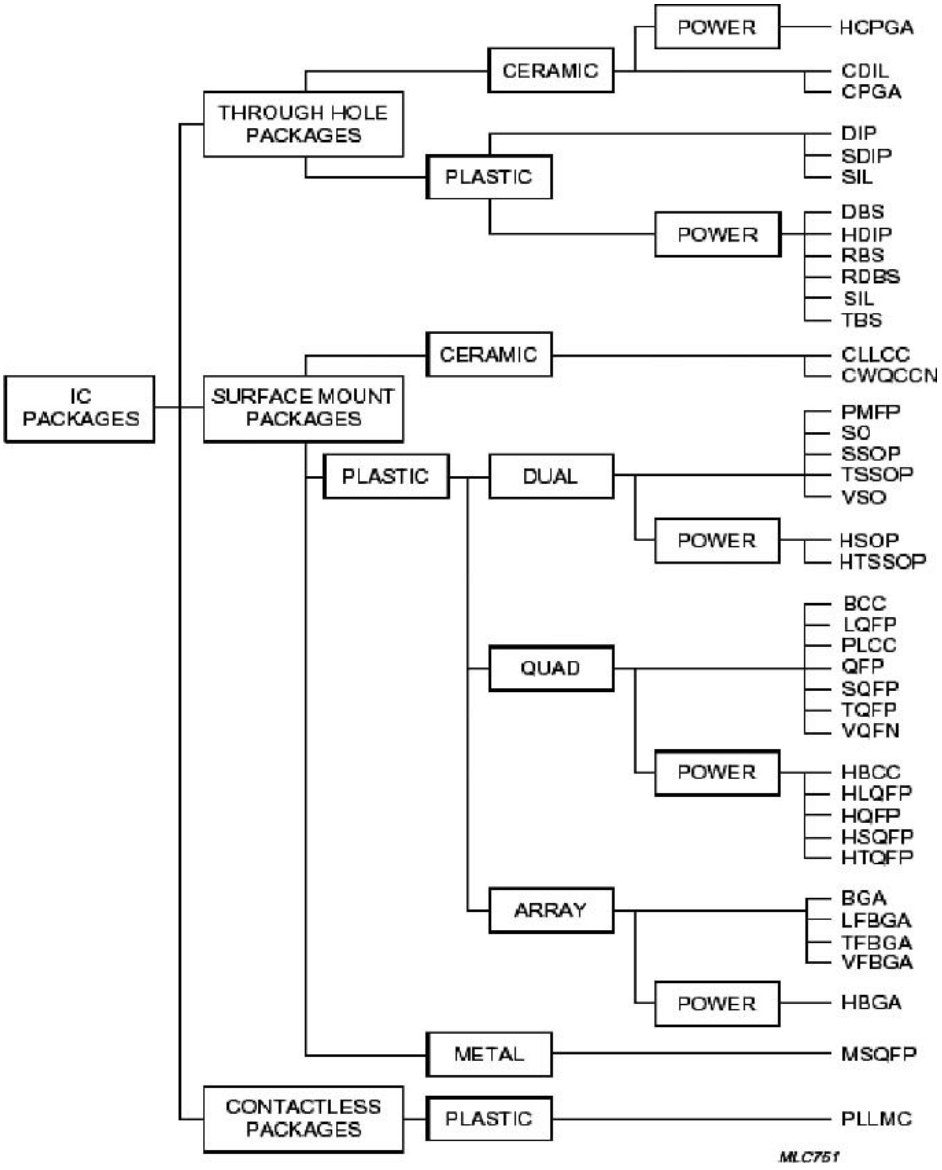

Figure 1.2 Classification of different packages

Figure 1.3 shows a schematic diagram of the assembly process involving a typical lead frame package. Packages are manufactured after a series of process one at a time using polymers in various forms.

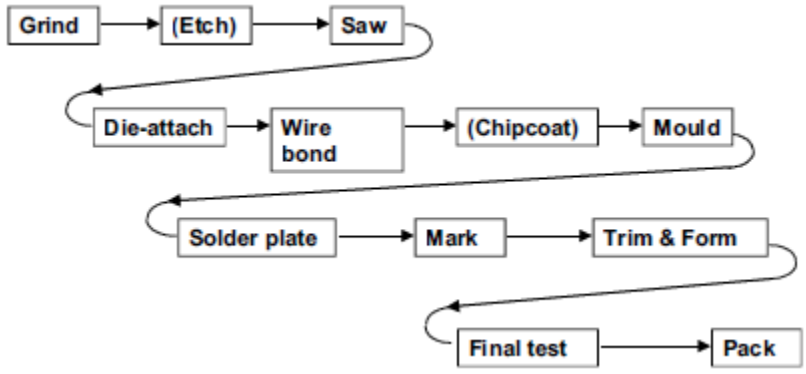

Figure 1.3 Schematic diagram of the assembly process of a lead frame package

1.2 Quad Flat No-Lead (QFN) Packages

The QFN package is a thermally enhanced standard size IC package designed to eliminate the use of bulky heat sinks and slugs. QFN is a leadless package where the electrical contact to the printed circuit board (PCB) is made through soldering of the lands underneath the package body rather than the traditional leads formed along the perimeter [2]. This package can be easily mounted using standard PCB assembly techniques and can be removed and replaced using standard repair procedures. The QFN package is designed such that the thermal pad (or lead frame die pad) is exposed to the bottom of the IC.

This configuration provides an extremely low resistance path resulting in efficient conduction of heat between the die and the exterior of the package (see Figure 1.4).

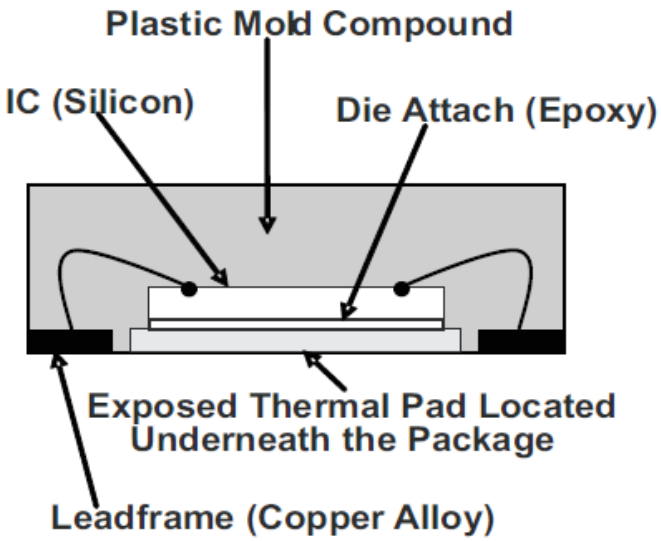

Figure 1.4 Cross section of a typical QFN package

Due to its superior thermal and electrical characteristics, this device package has gained popularity in the industry during the last couple of years. Due to its compact size, QFN package is an ideal choice for handheld portable applications and where package performance is required.

For this project, the QFN packages were obtained from Texas Instruments (TI) for analysis. The type of QFN and its details will be discussed in Chapter 5.

1.3 Board Level Reliability (BLR) Industry Standards

Reliability can be defined as the ability of a system or component to perform its required functions under stated conditions for a specified period of time. To quantify reliability, “ability” should be interpreted as a “probability”. From this definition it is clear that all products always fail eventually. Indeed, a probability of zero failure during a certain amount of time is physically impossible, even for integrated circuit (IC) [1].

There are many indicators used to describe reliability and one of the most widely used is the failure rate. If a plot of failure rate versus time is depicted, a curve in the shape of a bathtub cross-section is obtained as shown in Figure 1.5. Hence it’s widely referred to as a bathtub curve.

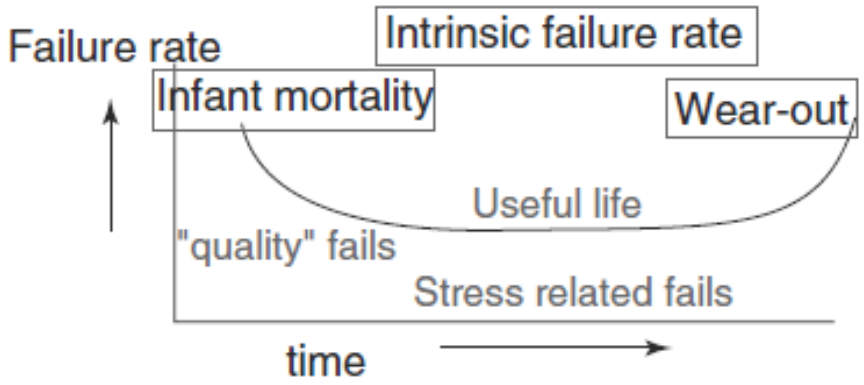

Figure 1.5 The bathtub curve: failure rate versus time

Three distinct phases of time can be seen in the bathtub curve: infant mortality, intrinsic failure and wear-out. Infant mortality or early failure is the period of time in which the product experiences failures also exclusively due to defects in the fabrication or assembly of the product. The intrinsic failure region has a near constant rate of failure since the poorly manufactured parts and defects were already screened out and eliminated and the majority of the population left are robust product which will enjoy long and sustained period where failures occur randomly. Finally, as the product ages, chemical, mechanical, or electrical stresses begin to weaken the product's performance to the point of failure. This is called the wear-out region.

To estimate the reliability of the package, environmental stress test are used to simulate the end use environment conditions and to uncover specific materials and process related marginalities that may be experienced during operational life. Few consortiums such as Joint Electronic Device Engineering Council (JEDEC) and Institute for Printed Circuits (IPC) have adapted, documented and standardized many of the reliability tests. Since the scope of this work is only during thermal cycling, we'll briefly discuss about it. Table 1.1 shows different temperature ranges for various service environments for electronic products.

Thermal cycling is used to simulate both ambient and internal temperature changes that result during device power up, operation and ambient storage in

controlled and uncontrolled environments. Due to difference in coefficient of thermal expansion between various package components, they warp and expand unevenly resulting in generation of internal thermal stresses which results in crack propogation in dielectric, fatigue and adhesion problems. These thermo-mechanical behaviors can be detected during thermal cycling tests. For reliability assessment, Weibull distribution is most commonly used to accurately reflect the behavior of the product in terms of failure rate.

Table 1.1 Thermal environments for electronic products

Use condition	Thermal excursion (°C)
Consumer electronics	0 to 60
Telecommunications	-40 to 85
Commercial aircraft	-55 to 95
Military aircraft	-55 to 125
Space	-40 to 85
Automotive-passenger	-55 to 65
Automotive-under the hood	-55 to 160

These reliability tests are either focused on package level or board level. Package level or 1st level reliability tests are dedicated to the robustness of the package component materials and design to withstand extreme environmental conditions and does not consider the interconnects when it is mounted on board.

Whereas for the board level or 2nd level reliability tests, stresses are examined on the solder joint of the surface mount package when mounted on board [3].

1.4 Objective

1.4.1 Motivation

QFN package gained popularity among the industry due to its low cost, compact size and excellent thermal electrical performance characteristics. Although QFN package is widely used in handheld devices, some customers require it for heavy industry application demanding thicker PCB. Literature suggests that as the thickness of PCB increases, the reliability and fatigue life of the package decreases since the board becomes stiffer and less flexible resulting in more transfer of stresses on the solder joint.

A 40 pin QFN RHM board of thickness 2.38mm (93mil), 8 layers was tested under accelerated thermal cycling (ATC) conditions for failure analysis (FA). The board was tested under varying temperature loads, first from 0°C to 100°C and then for another case from -40°C to +125°C, both times keeping the ramp and dwell time same (60min, 15min dwell). The tests showed that some units failed at 860 cycles and the board was removed at 1156 cycles for FA.

Another RHM QFN package with 3.4mm (134mil) thick board was tested under ATC conditions. The ATC profile was from -40°C to +125°C with 30min dwell and 8min ramp, using the IPC9592 standard. The test results showed that

out of 75 units on the board, 10 units showed early fails (less than 700 cycles) having insufficient joints, zero standoff or a combination of both (see Figure 1.6 and Figure 1.7).

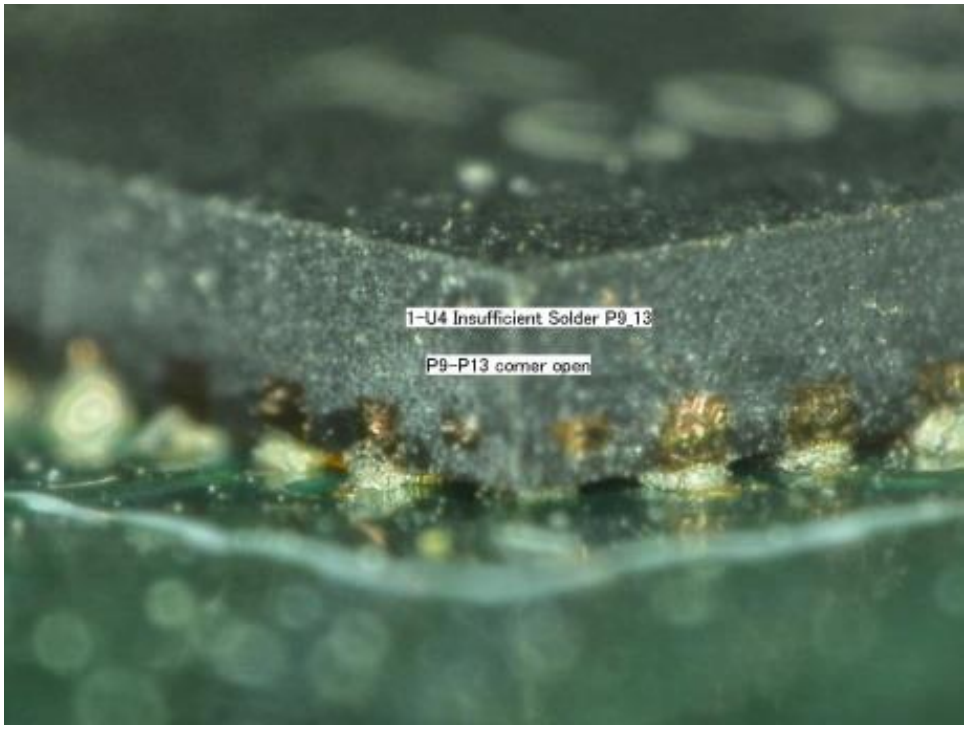

Figure 1.6 Typical fail unit showing insufficient joint

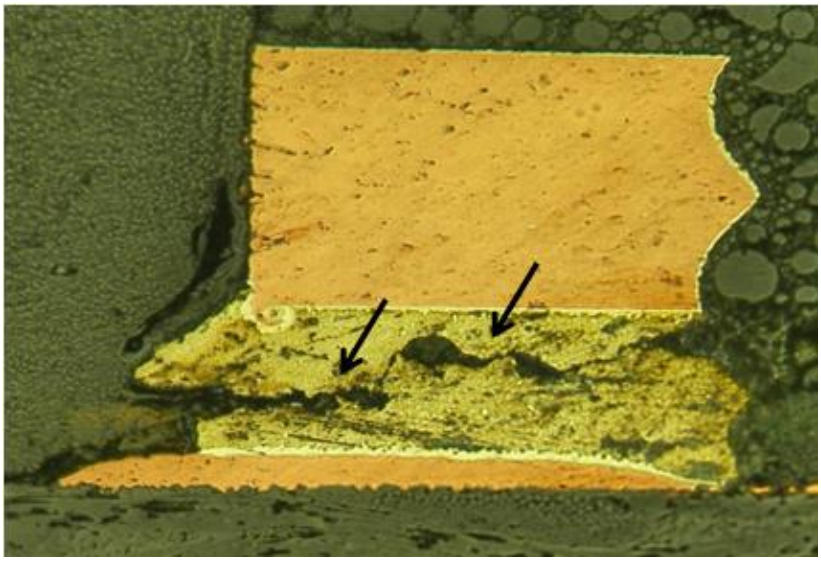

Figure 1.7 Crack propogation in a solder joint

From the test results of the two QFN packages, we can observe that the package on the thicker board fails much earlier than the thinner board. The failures detected on thicker board reduce the mechanical reliability of the package. This provides the motivation for this work. The thesis covers the analysis to understand the physics of failure in the package on thicker board and means to mitigate it, thus improving its reliability.

1.4.2 Goals and Objective

The primary objective of this work is to analyze the failures observed in the QFN package with thick FR4 board under ATC condition. Understand the root cause of the solder joint failures and methods to improve the mechanical reliability of the package thus making it to qualify the BLR industry standard for customers use.

Finite Element Analysis (FEA) is used to determine the fatigue correlation parameters such as strain energy density and plastic strain range. These parameters are a measure of the energy dissipated through plastic and creep deformation which is related to the damage done to the solder joint. Using these parameters, various energy based and strain based life prediction models are examined. The compatibility of these fatigue models for the QFN package is demonstrated. Furthermore, a methodology to derive a new power equation for QFN package family is shown in this study to accurately predict the characteristic life. Best design practices are demonstrated for FEA modeling to predict the solder joint reliability with minimal error.

Finally the effect of several key package components on the solder joint reliability is studied. The aim is to vary the parameters in an attempt to improve the board level reliability of the QFN package on thick FR-4 boards.

Chapter 2

LITERATURE REVIEW

Tong Yan Tee et al. [4] studied the board level solder joint reliability for both QFN and enhanced design of PowerQFN under thermal cycling. They established a detailed solder joint fatigue model with life prediction capability within ±34% error. They also performed a comprehensive design analysis to study the effects of key variables on fatigue life and suggested to have smaller package type, more center pad soldering, smaller die size, thinner die, bigger die pad size, thinner board, longer lead length/width, smaller pitch, higher solder standoff, solder with fillet, higher mold compound CTE and smaller temperature range of thermal cycling test for enhanced solder joint reliability of QFN. Their analysis found out that the land size, mold compound modulus and die attach material has insignificant effects on reliability.

Syed et al. [5] conducted series of experiments on QFN packages and provided guidelines on board design and surface mounting of this package. They also evaluated board level reliability for temperature cycling and recommended having mold compound with higher coefficient of thermal expansion (CTE), lower die to package size ratio, larger land size, thinner board, soldered exposed pad, slower ramp rate and lower temperature extremes and greater standoff height will enhance board level reliability and increase cycles to failure.

Birzer et al. [6] performed board level stress tests of QFN packages under temperature cycling, drop, bend and power cycling tests. They observed that the QFNs on thick boards with many metal layers are critical as compared to thin boards regarding temperature cycling reliability. Also, apart from the board thickness; board design, materials and surface mount technology (SMT) process has significant influence on the board level reliability of QFN packages.

Li Li et al. [7] developed a parametric 3D FEA model of QFN for board level reliability modeling and testing having the capability of predicting the fatigue life of solder joint during thermal cycling test within a certain error range. They also performed design for reliability and assembly analyses to study the effect of key parameters and use those results to develop best practice design and assembly recommendations.

Vries et al. [8] did a solder joint reliability analysis of selected series of small, medium and large HVQFN packages under thermal cycling using experimental, analytical and numerical solutions. They demonstrated the importance of board parameters such as the coefficient of thermal expansion and stiffness (board thickness and Young's modulus). Also the paper established that if the glass transition temperature (T_g) of the board enters between the thermal cycling range, the mechanism of building up of stress changes effecting the board level reliability.

Wei Sun et al. [9] tested various types of QFN packages and discussed the effects of surface mount techniques such as solder pad and stencil designs on solder joint reliability. They also examined the Schubert's fatigue model to predict the fatigue life and established a new power equation based on strain energy density and experimental results to predict the solder joint reliability within ±20% error.

Stoeckl et al. [10] identified the most sensitive parameters of VQFN packages and studied its effects on the solder joint reliability. The parameters included the material properties, component design and the board layup. They also modified the Darveaux's crack growth constant for the VQFN package to achieve good correlation between simulation and test results. Using this modified Darveaux's model, the fatigue life can be predicted within a 2X accuracy range with test results.

Chapter 3

DESIGN FOR RELIBAILITY (DFR) METHODOLOGY

The primary objective of this work is to understand and mitigate the root cause of the solder joint failure and provide guidelines to improve the fatigue life of the package. The methodology described in this chapter is leveraged to meet this objective. Fundamentally, DFR of electronics packages consists of three parts:

- Experimental methods for reliability tests
- FEA modeling and simulation
- Fatigue life prediction analysis

Figure 3.1 shows the DFR methodology flowchart.

The reliability testing for thermal cycling provides the actual failure mechanism of special design of electronic packaging which can be further used to correlate with the results of FEA modeling and solder fatigue life prediction analysis. Reliability testing on all QFN packages was conducted by Texas Instruments.

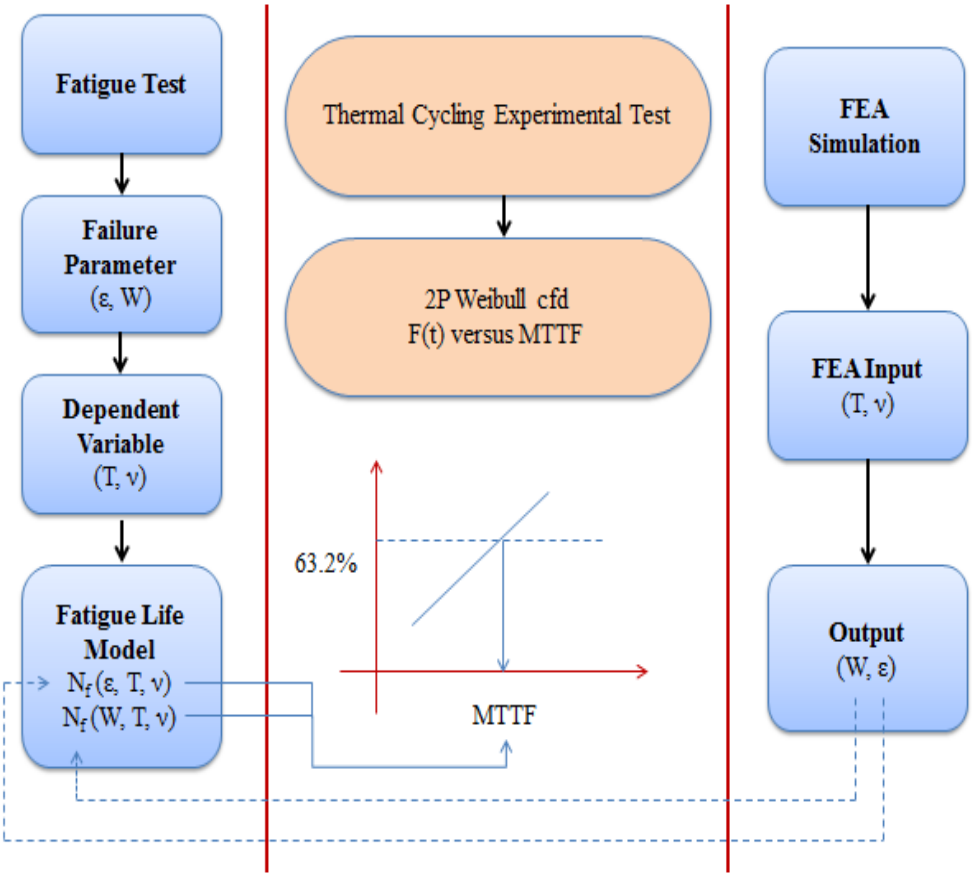

Figure 3.1 DFR methodology flowchart

Finite element method is applied to investigate the QFN solder joint reliability modeling. This simulation involves five main input parameters: 1) material property, 2) geometry, 3) boundary conditions, 4) meshing and 5) initial and loading conditions. For eutectic solder materials, Anand's model is applied to describe the visco-plastic behavior. The rest of the materials are assumed to be linear elastic. FR4 board is considered to be orthotropic having different in-plane

and out-of-plane properties. Quarter symmetric model of QFN is considered for simulation and sub-modeling technique is used for accurate analysis. Thermal loading conditions were followed using IPC9592 [11] standard for over three complete cycles. Average plastic work (strain energy density) and plastic strain is determined after each cycle which is further used in the solder fatigue life models. Furthermore, mesh sensitivity analysis is performed on the critical solder to study its effects on the results.

Initially different fatigue life prediction models are examined to determine the characteristic life. The test vehicle used for the simulation is a 6x6mm QFN package on 93mil board. Different element layers of the critical solders are examined for volume averaging and the best practice method is proposed. Based on the simulation data and the BLR test results, a new power equation is derived to accurately predict the fatigue life of the QFN package.

Additionally, design analysis of QFN package is performed to study the effect of key package components on the solder joint reliability. The test vehicle used for this study is a 6x6mm QFN package on 134mil board. Only one package parameter is modified at a time to study the effects of each parameter on the reliability of the package.

Chapter 4

FINITE ELEMENT MODELING

4.1 Introduction to Finite Element Method

The Finite Element Method is a computational technique used to obtain approximate solution to boundary value problem in engineering. FEM is virtually used in almost every industry that can be imagined. Common application of FEA applications are mentioned here.

- Aerospace/Mechanical/Civil/Automobile Engineering
- Structural Analysis (Static/Dynamic/Linear/Non-Linear)
- Thermal/Fluid Flow
- Nuclear Engineering
- Electromagnetic
- Biomechanics
- Geomechanics
- Biomedical Engineering
- Hydraulics
- Smart Structures

"The Finite Element Method is one of the most powerful numerical techniques ever devised for solving differential equations of initial and boundary value problems in geometrically complicated regions" [12]. Sometimes it is hard

to find analytical solution of important problems as they come with complicated geometry, loading condition, and material properties. So FEA is the computational technique which helps in reaching the satisfactory results with all the complex conditions that can't be solved through analytical procedure. There are wide range of sophisticated commercial code available which helps in reaching the approximately close solution in 1D, 2D and 3D. In this FEA method, the whole continuum is divided into a finite numbers of small elements of geometrically simple shape. These elements are made up of numbers of nodes. Displacement of these nodes is unknown and to find it, polynomial interpolation function is used. External force is replaced by an equivalent system of forces applied at each node. By assembling the mentioned governing equation, results for the entire structure can be obtained.

$\{F\} = [K]\{u\}$

Where, $\{F\}$ = Nodal load/force vector

$[K]$ = Global stiffness matrix

$\{u\}$ = Nodal displacement

Structure's stiffness (K) depends on its geometry and material properties. Load (F) value has to be provided by user. The only unknown is displacement (u). The way in general FEA works is, it creates the number of small elements with each containing few nodes. There are equations known as Shape function in software, which tells software how to vary displacement (u) across the element

and average value of displacement is determined at nodes. Those stress and/or displacement values are accessible at nodes which explains that finer the mesh elements, more accurate the nodal values would be. So there are certain steps that we need to follow during the modeling and simulation in any commercial code to reach approximately true solution, which would be explained hereby [13]. In this study commercially available FEA tool, ANSYS Workbench v15.0 has been leveraged.

4.2 FEA Problem Solving Steps

These five steps need to be carefully followed to reach satisfactory solution to FEA problem:

1) Geometry and Material definition
2) Defining Connection between bodies
3) Meshing the model
4) Defining load and boundary condition
5) Understanding and verifying the results

ANSYS is a general purpose FEA tool which is commercially available and can be used for wide range of engineering application. Before we start using ANSYS for FEA modeling and simulation, there are certain set of questions which need to be answered based on observation and engineering judgment. Questions may be like what is the objective of analysis? How to model entire physical system? How much details should be incorporated in system? How

refine mesh should be in entire system or part of the whole system? To answer such questions computational expense must be compared to the level of accuracy of the results that needed. After that ANSYS can be employed to work in an efficient way after considering the following:

- Type of problem
- Time dependence
- Nonlinearity
- Modeling simplification

From observation and engineering judgment, analysis type has to be decided. In this study the analysis type is structural; to be specific out of different other structural problem focus in this study is on Static analysis. Non-linear material and geometrical properties such as plasticity, contact, and creep are available.

4.2.1 Geometry and Material Definition

Geometrical nonlinearity needs to be considered before analysis. This nonlinearity is mainly of two kinds.

1) Large deflection and rotation: If total deformation of the structure is large compared to the smallest dimension of structure or rotate to such an extent that dimensions, position, loading direction, change significantly, then large deflection and rotation analysis becomes necessary. Fishing rod explains the large deflection and rotation.

2) Stress Stiffening: Stress stiffening occurs when stress in one direction affects the stiffness in other direction. Cables, membranes and other spinning structures exhibit stress stiffening.

Material nonlinearity is also the critical factor of FE analysis, which reflects in the accuracy of the solution. If material exhibit linear stress-strain curve up to proportional limit or loading in a manner is such that it doesn't create stress higher than yield values anywhere in body then linear material is a good approximation. If the material deformation is not within the loading condition range is not linear or it is time/temperature dependent then nonlinear properties need to be assigned to particular parts in system. In that case plasticity, creep, viscoelasticity need to be considered. Apart from that if structure exhibit symmetry in geometry, then it needs to be considered when creating model of physical structure which is advantageous in saving the computational time and expense [14]. Once the geometry and material properties are taken care of contacts between different bodies needs to be considered such as rigid, friction, bonded etc.

4.2.2 Meshing Model

As discussed in section 4.1, large number of mesh counts (elements) provides better approximation of solution. There are chances in some case that excessive number of elements increases the round off error. It is important that mesh is fine or coarse in appropriate region and answer to that question is

completely dependent on the physical system being considered. In some cases mesh sensitivity analysis is also considered to balance computational time with accuracy in solution. Analysis is first performed with certain number of elements and then with twice the elements. Then both the solutions are compared, if solutions are close enough then initial mesh configuration is considered to be adequate. If solutions are different than each other then more mesh refinement and subsequent comparison is done until the convergence is achieved [15]. There are different types of mesh elements for 2D and 3D analysis in ANSYS which can be used based on application.

4.3 Sub modeling

To get the most accurate results in region of interest out of your whole system sub modeling technique is used. In FE analysis it may occur that mesh is too coarse to provide satisfactory results in the area of interest where stress in higher. Sub modeling is sometimes known as global-local analysis or cut boundary displacement method. Cut boundary is the boundary of the sub model where it has been cut through global model. Displacement calculated on the boundary of the cut from global model is applied as a boundary condition for the sub model at cut boundary planes. Figure 4.1 explains how area of interest (high stress) from global model of pulley hub and spokes is differentiated in sub model.

St. Venant's principle supports sub modeling technique. It states that if actual force distribution is replaced by statically equivalent system, the

distribution of stress and strain is altered only near the region of load application. This explains that stress concentration effects are localized around the concentration, so if the boundary of the sub model is far enough away from the area of interest, reasonably accurate results can be calculated in the sub model.

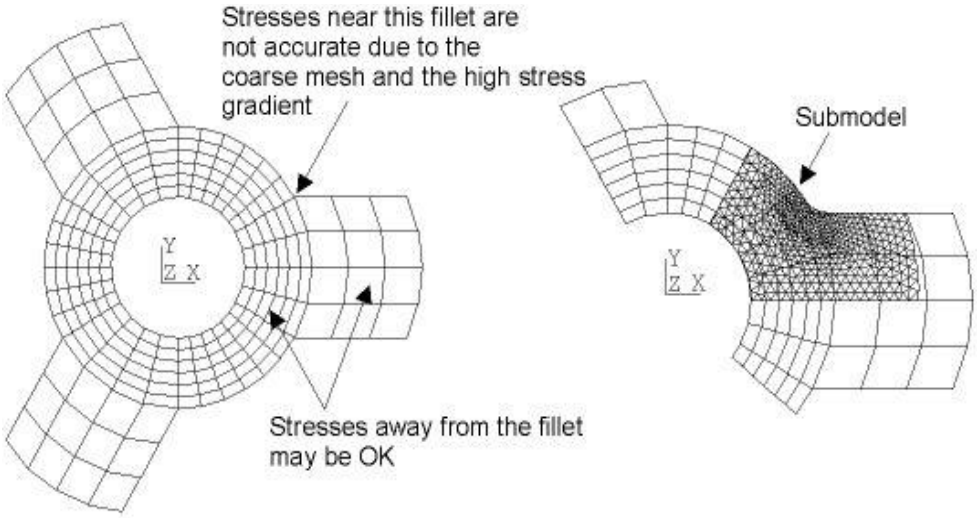

Figure 4.1 Concept of sub modeling

Apart from just the accuracy there are other benefits of sub modeling, which are stated here below:

- The need for transition region in solid FE models is reduced or eliminated.
- It allows you to experiment on different design and area of interest.
- It helps you in getting adequate mesh refinement.
- You can independently tackle sub model, even geometry modification or improvement can also be done.

Chapter 5

FINITE ELEMENT ANALYSIS AND SIMULATION

5.1 Modeling of QFN Package

This chapter reports the application of FEA modeling and simulation techniques used for the QFN package assembly design-for-reliability (DFR). The ANSYS FEA procedures consist of three steps.

1. Preprocessing: Create geometric model, elements and mesh, input material properties.
2. Solution Process: Apply loads and boundary condition, output control, load step control, selecting proper solver, obtaining the solution.
3. Post processing: Review the result; list the result, contour map, result animation.

Certain assumptions have been made to carry out finite element analysis.

- All the parts in 3D package is assumed to be bonded to each other
- Temperature change in package during thermal cycling is assumed to be same throughout the package
- Except solder bump, all other materials are assumed to behave as linear elastic

5.2 Package Geometry

A 3D 6 x 6mm QFN package was modeled in ANSYS v15.0 [16] using the package drawings and optical microscope images. Figure 5.1 and Figure 5.2 shows the cross-sectioning of the QFN package and X-ray images highlighting the major components respectively. The daisy chains are clearly visible in the X-ray images. Figure 5.3 shows the daisy chain along with the pin numbers. Figure 5.4 shows the package outline and configuration.

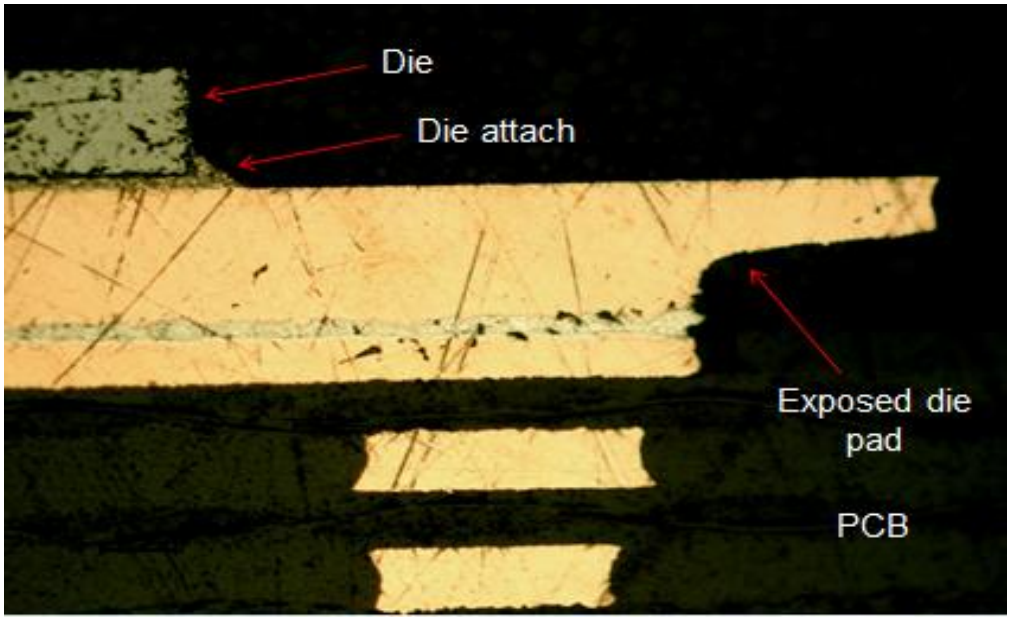

Figure 5.1 Cross section of QFN assembly

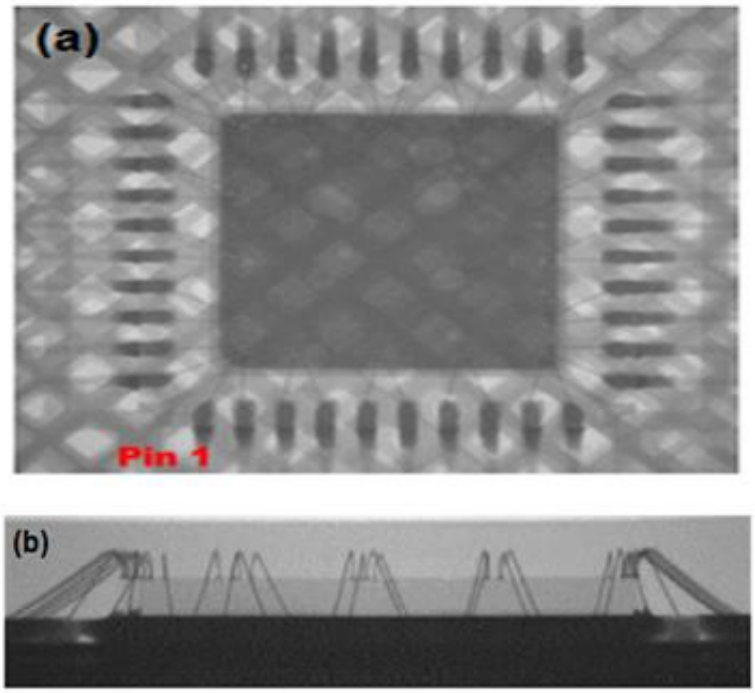

Figure 5.2 X-ray of assembled package (a) Top view (b) Front view

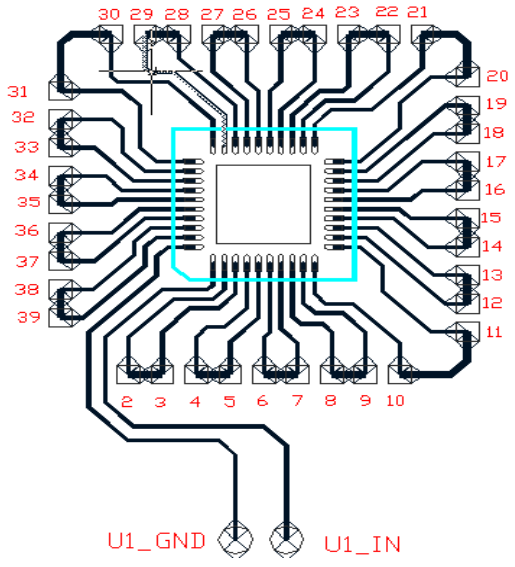

Figure 5.3 Daisy chain of QFN package

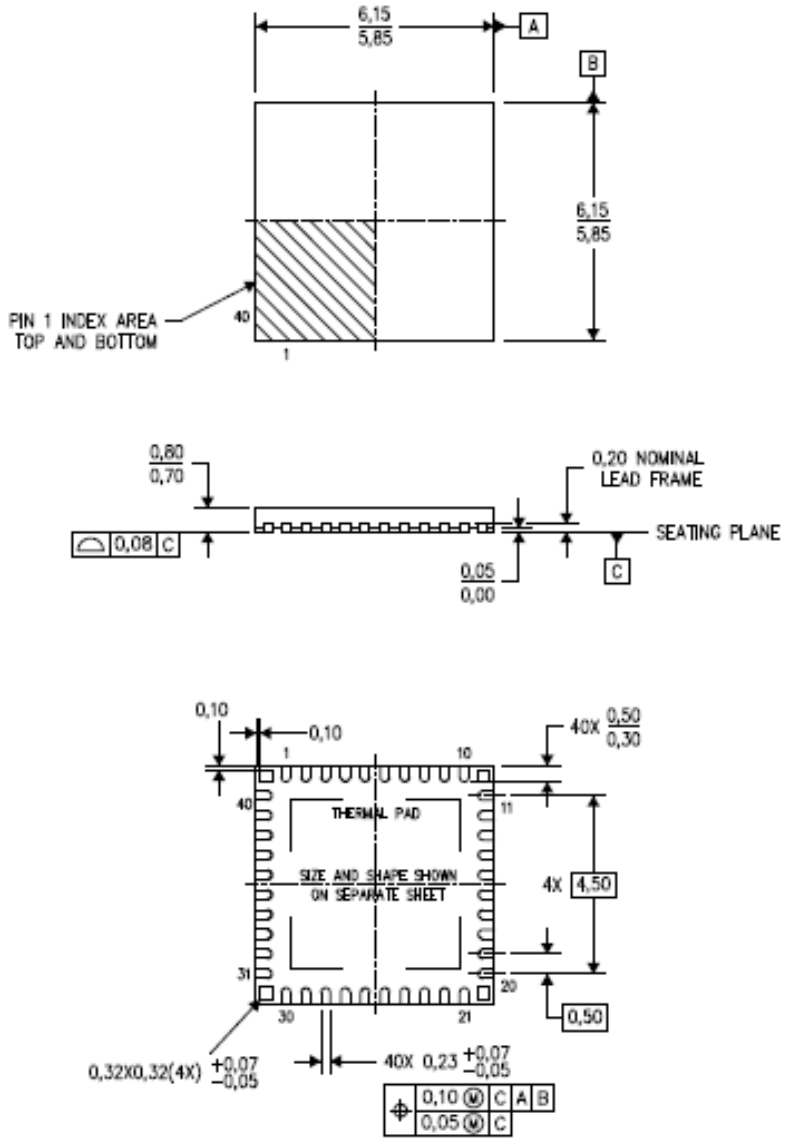

Figure 5.4 QFN package configuration (mm)

Figure 5.5 shows the exposed pad dimensions. This exposed thermal pad is designed to be attached directly to the PCB. The thermal pad is soldered directly to the PCB such that the PCB itself can be used as a heatsink.

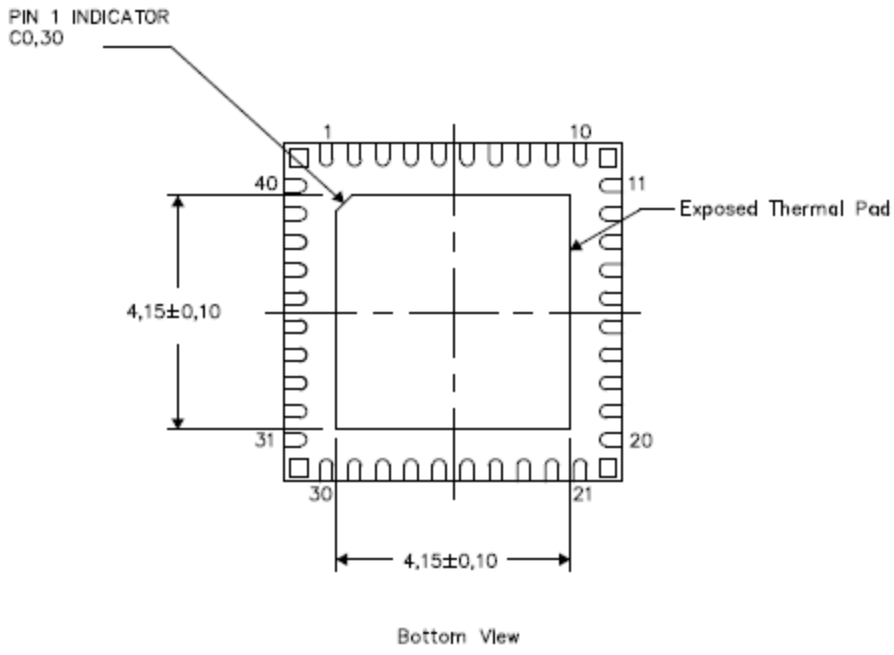

Figure 5.5 Exposed thermal pad dimensions

Figure 5.6 shows a 3D quarter geometry of 6 x 6mm QFN package. Quarter model is considered to save computational time without affecting the accuracy of the results. Symmetric conditions are applied on the two faces as shown in the diagram. Figure 5.7 shows the detailed view of the package components. Mold compound is kept hidden for the visibility of the other package components.

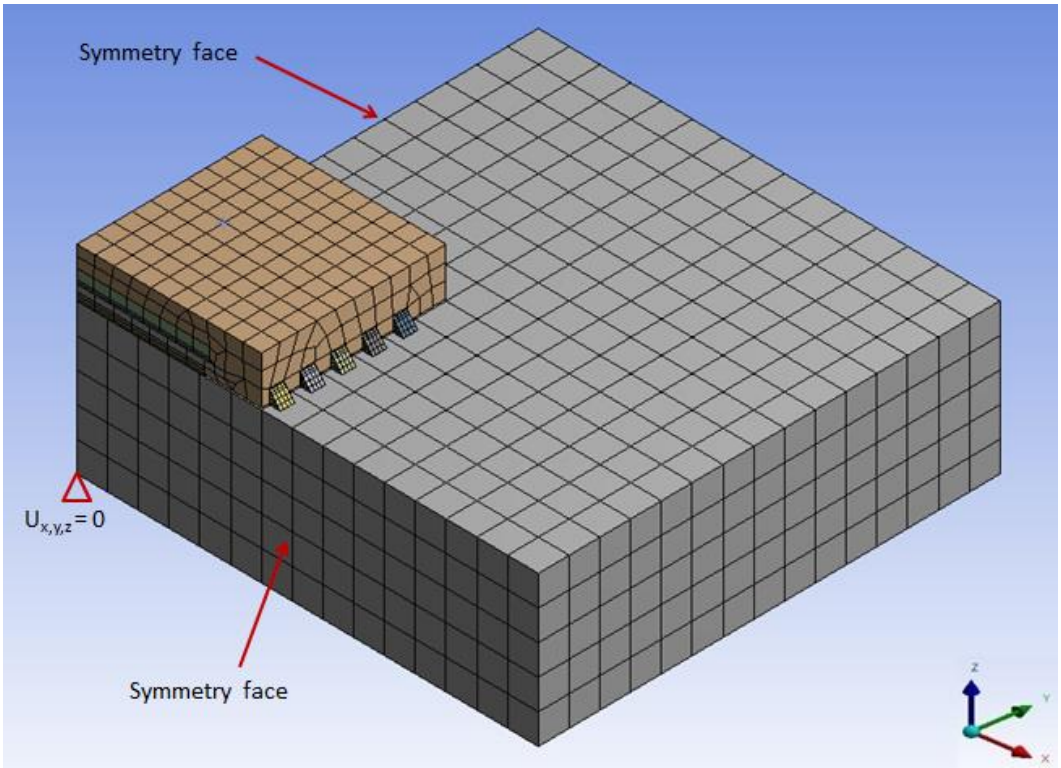

Figure 5.6 3D quarter global model

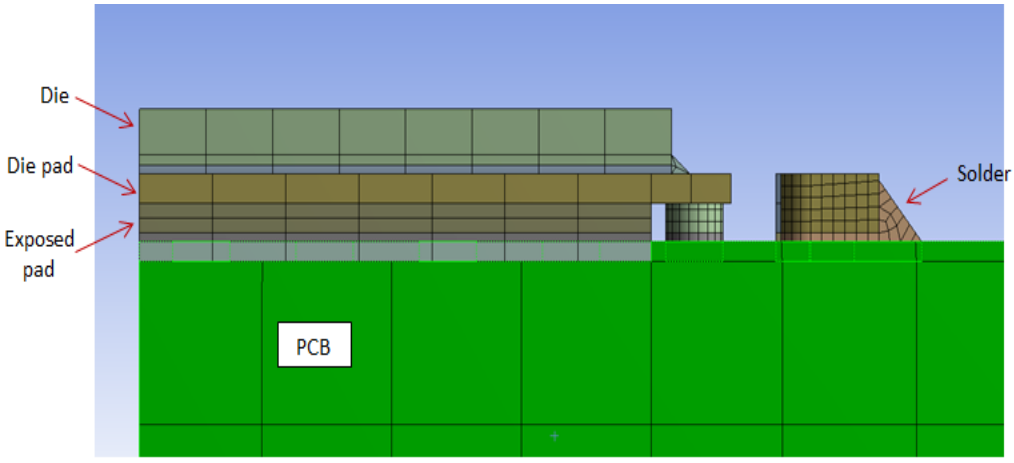

Figure 5.7 Detailed view of global model

Table 5.1 shows the dimensions of the global model and package components.

Table 5.1 Package component dimensions

Component	Dimensions (mm)
Package	6 x 6 x 7.5
Die	4.315 x 3.245 x 0.19
Die Pad	4.8 x 4.8 x 0.1
Exposed Thermal Pad	4.15 x 4.15 x 0.1
Solder Thickness	0.3
Anchor Pin	0.32 x 0.32 x 0.2
Pitch	0.5
PCB	15 x 15 x 2.38
	15 x 15 x 3.45

5.3 Sub Modeling

Global–Local modeling (Sub modeling) technique is needed when the 3D model is too large to solve or when the loading on the assembly does not have any axes of symmetry and a full 3D model is needed. The method employs a coarser global model, which is able to capture the 3D effect of deformations on a selected local sub model assembly. Transfer of the corresponding elastic deformations to a finer local sub model is used to perform a detailed nonlinear strain analysis in a

solder joint. An effective finite element method was proposed by Yu et al. [17] to analyze the stress of the leads and the solder joints in the surface-mount assembly (SMA). Using this technique more efficient results in the local region of the model can be obtained.

Sub modeling technology is based on St. Venant's principle, which states that if an actual distribution of forces is replaced by a statically equivalent system, the distribution of stress and strain is altered only near the regions of load application. This implies that stress concentration effects are localized around the concentration; therefore, if the boundaries of the sub model are far enough away from the stress concentration, reasonably accurate results can be calculated within the sub model region. Aside from the obvious benefit of giving more accurate results in a region of model, the sub modeling technique can reduce, or even eliminate, the need for complicated transition regions in solid finite element models.

The 3D quarter model (Figure 5.6) is analyzed using relatively coarse mesh model. The region of interest i.e. the critical solder is identified and a sub model is created as shown in Figure 5.8. The procedure to identify the critical solder is explained in detail in the next chapter. Cut boundary interpolation is performed in sub modeling such that the global model displacement field is used to define boundary condition in local model (see Figure 5.9). The nodes along the cut boundaries firstly are identified and then the program calculates the degree of

freedom (DOF) values at those nodes by interpolating results from the full (coarse) model. For each node of the sub model along the cut boundary, the program uses the appropriate element from the coarse mesh to determine the DOF values. These values are interpolated onto the cut boundary nodes using the element shape functions.

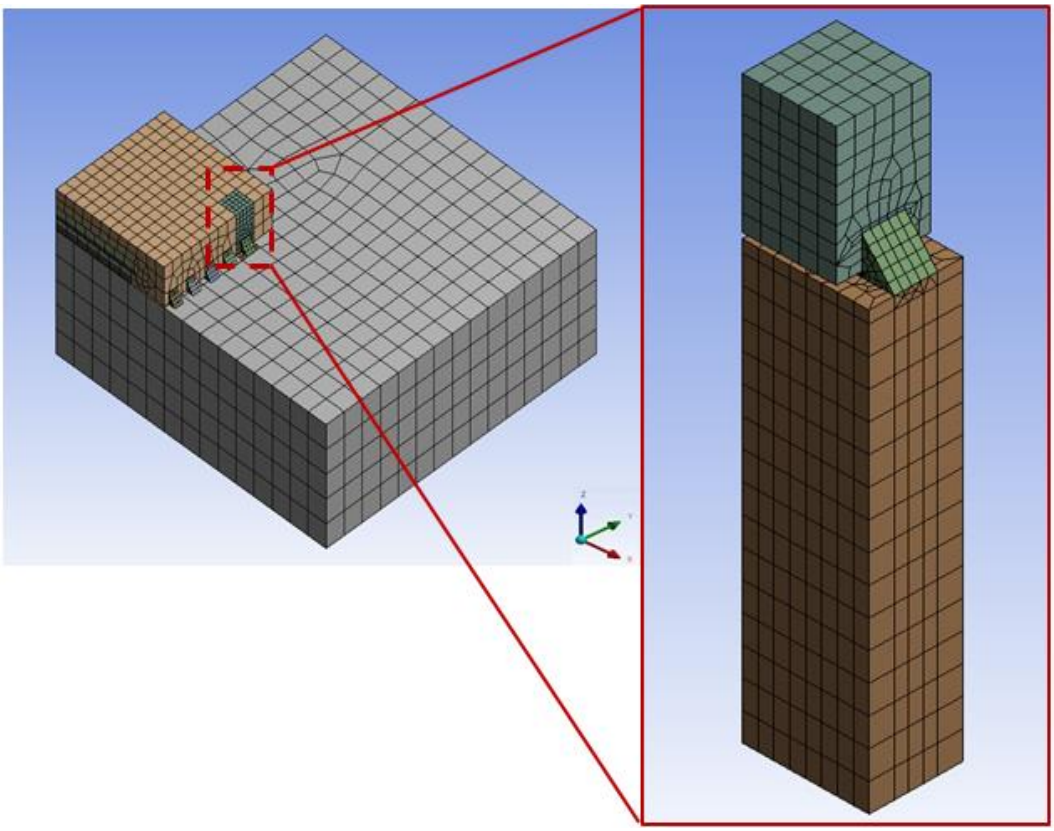

Figure 5.8 Global model and sub model

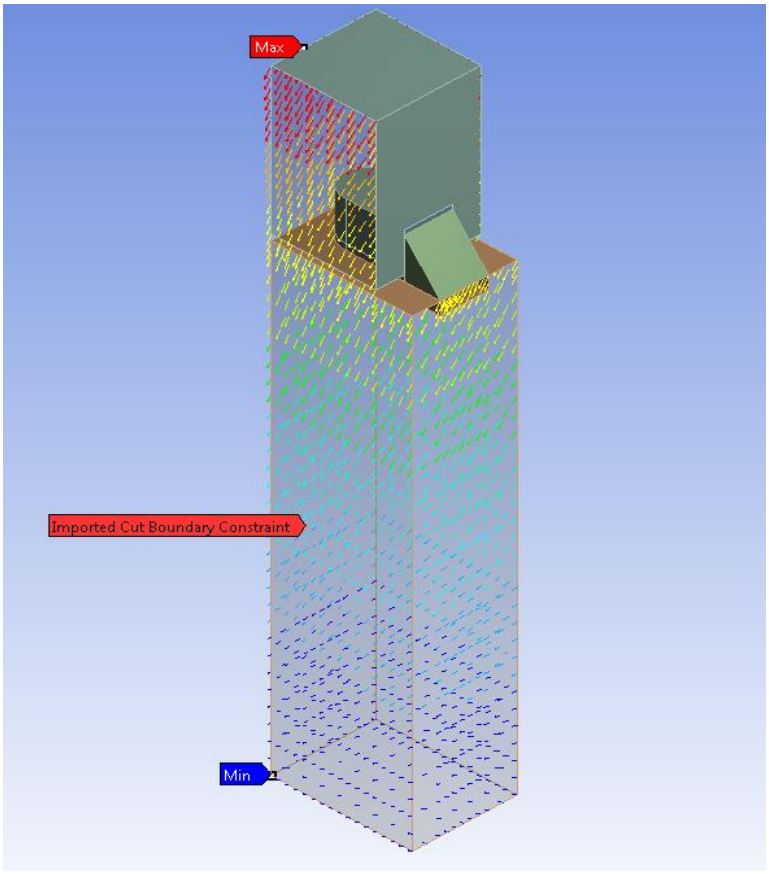

Figure 5.9 Cut boundary interpolation

5.4 Meshing, Boundary Condition and Thermal loadings

The global model was discretely meshed using different meshing option in ANSYS Workbench v15.0. Special meshing operations were carried out to make sure that model has mesh continuity throughout the thickness of package in the very far corner unit cell as it is the region of interest. Rest part of the packages where meshed in such a way that, reasonable mesh continuity is achieved in less time so that reasonable response can be captured through nodal averaging in

ANSYS. Mesh refinement and mesh sensitivity analysis was performed in sub model to reach maximum accuracy.

Boundary conditions imposed on the global model can be seen in Figure 5.6. Symmetry boundary conditions are applied to the two boundary planes of the quarter symmetry model. The center node is fixed to prevent rigid body motion.

Two different thermal cycling conditions are used for simulations as shown in Table 5.2. The two temperature profiles are shown in Figure 5.10 and Figure 5.11. These simulations are done over three complete cycles since most of the solder joints have reached a stable state after the end of third cycle. The initial stress-free temperature was set to be the maximum temperature in the cycle. Choosing the high dwell temperature of the BLR test as the stress-free temperature helps the system to reach the stabilized state faster [18].

Table 5.2 Thermal cycle conditions

Name	Temperature range (°C)	Dwell (min)	Ramp (min)
TC1	-40 to +125	15	60
TC2	0 to +100	15	60

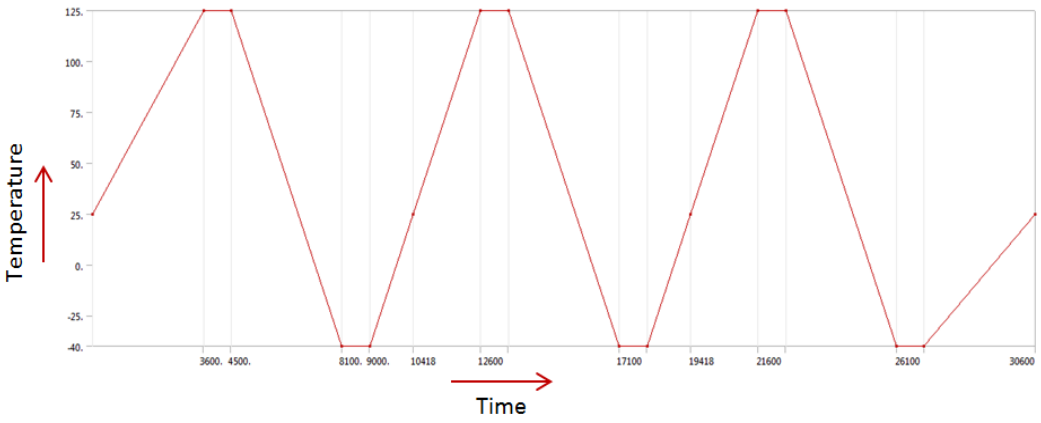

Figure 5.10 TC1 temperature profile

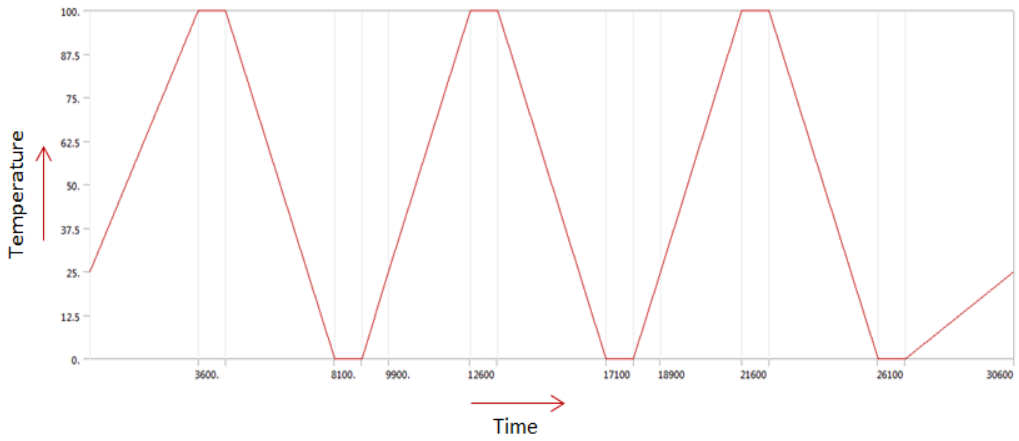

Figure 5.11 TC2 temperature profile

5.5 Material Properties

All material properties are taken as linear elastic and FR4 is considered as orthotropic having different in-plane and out-of-plane properties. Table 5.3 and Table 5.4 show the material properties of all package components. These properties were obtained from the vendor datasheets.

Table 5.3 Orthotropic properties of FR4

Young's Modulus (GPa)	Poisson's Ratio	Shear Modulus (GPa)	Coefficient of Thermal Expansion (ppm/°C)
E_x, E_y = 27.184 E_z = 11.884	ν_{xz}, ν_{yz} = 0.39 ν_{xy} = 0.11	G_{xz}, G_{yz} = 5.792 G_{xy} = 12.266	α_x,α_y = 16 α_z = 84

Table 5.4 Material properties of package components

Material	Young's Modulus (GPa)	Poisson's Ratio	Coefficient of Thermal Expansion (ppm/°C)
Die	131	0.278	2.61
Die Attach	11.8	0.3	64
Leadframe	129	0.34	17
Epoxy Mold Compound	3	0.3	63
Exposed Die Pad	129	0.34	17

SAC305 (96.5% tin, 3% silver, 0.5% copper) is used as the material for solder. Anand's viscoplastic constitutive law is used to describe the inelastic part of the lead-free solder. This constitutive law follows the materials perspective that

dislocation motion is the cause of both creep and plastic deformation, and combined them into inelastic strain [17].

The total strain is expressed as,

$$\varepsilon_{ij} = \varepsilon_{ij}^{e} + \varepsilon_{ij}^{in}$$

where ε_{ij}^{in} is the inelastic strain tensor.

The Anand's model consists of two coupled differential equations that relate the inelastic strain rate to the rate of deformation resistance.

The strain rate equation is represented by,

$$\frac{d\varepsilon_{in}}{dt} = A\left[\sin h\left(\xi\frac{\sigma}{s}\right)\right]^{\frac{1}{m}} \exp\left(-\frac{Q}{RT}\right)$$

The rate of deformation resistance is given by,

$$\dot{s} = \left\{h_0(|B|)^{\alpha}\frac{B}{|B|}\right\}\frac{d\varepsilon_p}{dt}$$

$$B = 1 - \frac{s}{s^*}$$

$$s^* = \hat{s}\left[\frac{1}{A}\frac{d\varepsilon_p}{dt}\exp\left(-\frac{Q}{RT}\right)\right]$$

where $\frac{d\varepsilon_{in}}{dt}$ is the effective inelastic strain rate, σ is the effective true stress, s is the deformation resistance, T is the absolute temperature, A is pre-exponential factor, ξ is stress multiplier, m is strain rate sensitivity of stress, Q is activation energy, R is universal gas constant, h_0 is hardening/ softening constant, $\hat{s}$ is coefficient for deformation resistance saturation value, n is strain-rate sensitivity

of saturation value, and a is strain-rate sensitivity of hardening or softening. Anand's viscoplasticity law consists of nine material constants and is listed in Table 5.5. These constants were determined by Texas Instruments at Purdue. The elastic part of the constitutive law of lead-free solder can be described by a temperature-dependent Young's modulus, Coefficient of thermal expansion and Poisson's ratio (ν=0.4). The temperature-dependent Young's modulus and Coefficient of thermal expansion is $E = 194T+100501$ (MPa) and $\alpha = 0.0022T^2 + 0.3951T + 7.4203$ (ppm/°C) respectively in which the absolute temperature T is in Degree Celsius.

Table 5.5 Anand's constant for SAC305 solder

Anand's constants	SAC305
s_0 (MPa)	2.15
Q/k (K)	9970
A(1/sec)	17.994
ξ	0.35
m	0.153
h_0 (MPa)	1525.98
$\hat{s}$ (MPa)	2.536
n	0.028
a	1.69

Chapter 6

RESULTS AND DISCUSSION

6.1 Fatigue Life Prediction Models for Solder

The solder joints subjected to thermal cycling load tend to fail in the Low Cycle Fatigue (LCF) range due to thermo-mechanical failure. The fatigue life to failure generally falls between 100 to 10,000 thermal cycles. Depending on the test conditions and the fatigue damage parameters used, the selection of fatigue life models are made. The fatigue damage driving force parameters such as the plastic strain-range, creep strain range and inelastic strain energy density per cycle are a good correlation index to the BLR lifetime [19] [20] [21].

The strain range-based fatigue approach employs low cycle strain-controlled fatigue test method. The inelastic strain comprises of the plastic strain range and creep strain range. The plastic shear strain deformation is represented by the time-independent plastic strain component, while the creep strain component contributes to the time-dependent inelastic strain included in the plastic shear strain ($\Delta\gamma_p$) component as shown in Figure 6.1. The energy-based fatigue model employs the cyclic stress–strain hysteresis loop to compute the elastic strain energy density (ΔW_e) and inelastic dissipated energy or plastic work per cycle (ΔW_p) [17].

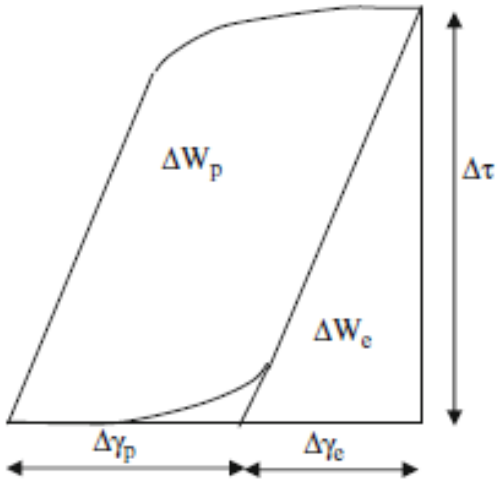

Figure 6.1 Cyclic stress-strain hysteresis loop

In this work, numerous fatigue models are examined to check its accuracy for QFN_RMH package with SAC305 solder joints. These fatigue models are discussed below.

6.1.1 Energy Based Model

Darveaux [19] and a lot other groups have shown that the increment of inelastic strain energy density per thermal cycle can be used as a fatigue indicator. The inelastic strain energy density (inelastic strain energy per unit volume) is defined by

$$W^{in} = \int \sigma_{ij}\, d\varepsilon_{ij}^{in}$$

where σ_{ij} is the stress tensor and ε_{ij}^{in} in is the inelastic strain tensor. Since we are using Anand's constitutive law for the solder, the inelastic strain in this case is the viscoplastic strain.

Wei Sun et. al. [9] derived a new curve fitted fatigue correlation model for QFN packages based on simulated accumulated creep strain energy density and corresponding thermal cycling experimental results (see Figure 6.2). The solder used in the packages were SnPb and Pb-free solder alloys. The equation is given by

$$N_{cha} = 741.37\, W_{acc}^{(-0.3902)}$$

where N_{cha} is the characteristic life (cycles to 63.2% failure) and W_{acc} (unit in megapascal) is the accumulated creep strain energy density per cycle.

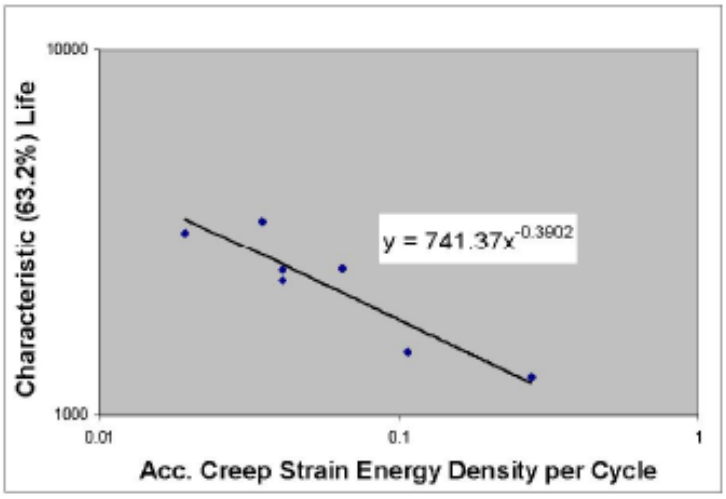

Figure 6.2 Wei Sun's energy based model for QFN

Note the inelastic strain in this case is the creep strain because Schubert's hyperbolic sine constitutive law was used to describe the solder material behavior.

Schubert [22] proposed a fatigue model based on dissipated energy density during one thermal cycle and characteristic life. The model was proposed for

PBGA's, CSP's and Flip-Chip packages for both SnPbAg and SnAgCu solder alloys (see Figure 6.3). In this work we will examine the model for SAC solder. The equation for the model is given by

$$N_f = 345\, W_{cr}^{(-1.02)}$$

where N_f is the characteristic life (cycles to 63.2% failure) and W_{cr} (unit in megapascal) is the strain energy density per cycle.

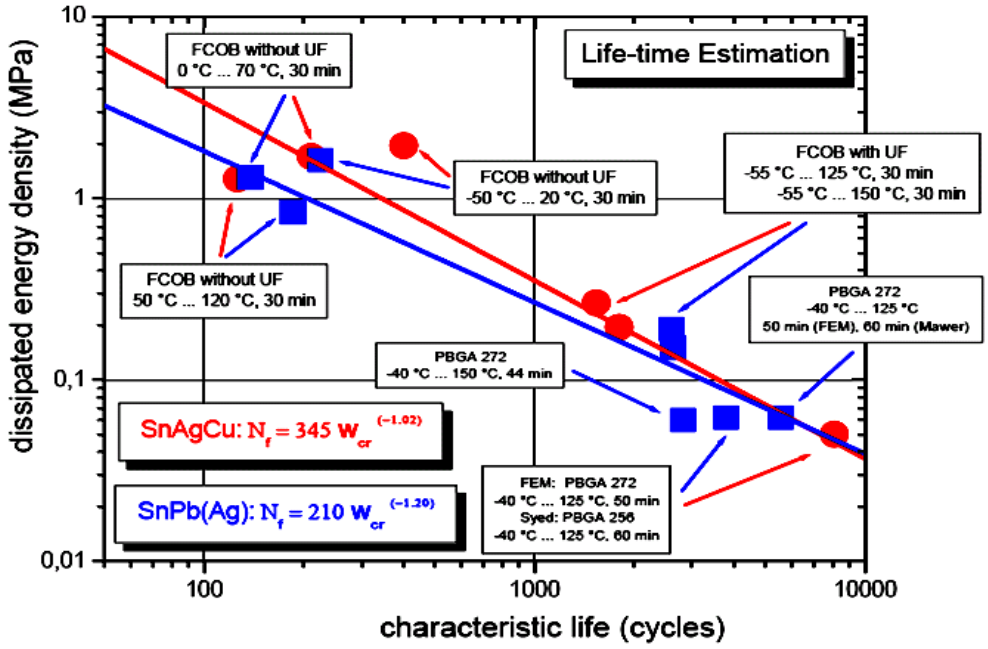

Figure 6.3 Schubert's energy based model for SAC and SnPb solder

Morrow's [23] energy based model is used predict the low cycle fatigue life N_f in terms of inelastic strain energy density W_p (MPa) as shown below

$$N_f^n W_p = A$$

where n is the fatigue exponent and A is material ductility coefficient. These constants were determined by Pang [24] for SnAgCu solder alloys which will be used in the Morrow's model in this study. For temperature 125°C and frequency 0.001Hz, the constants n and A were taken as 0.897 and 311.7 respectively.

Syed [25] determined a life prediction model for CSP's and BGA's with SnAgCu solder material using strain energy density (or plastic work). The equation for the model is written below (see Figure 6.4)

$$N_f = 674.08\Delta W^{(-0.9229)}$$

The unit for plastic work (ΔW) is MPa or its equivalent MJ/m^3.

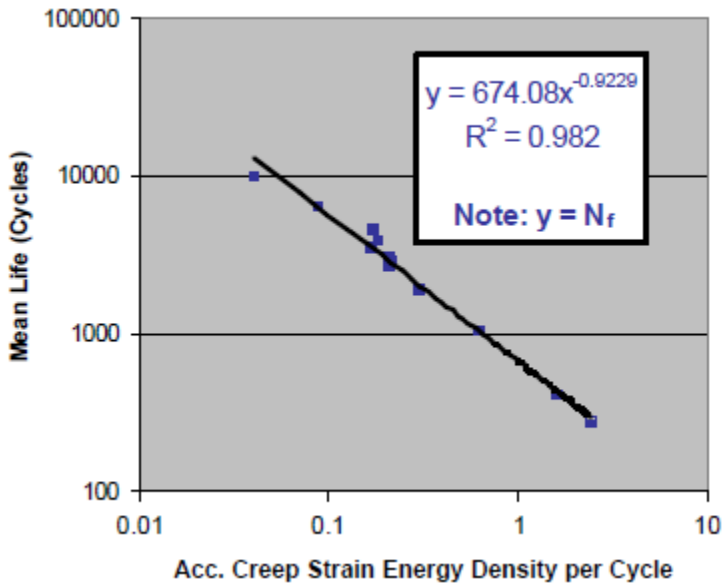

Figure 6.4 Syed's energy based model for CSP and BGA

6.1.2 Plastic Strain Range Fatigue Models

The Coffin-Manson [20] [21] fatigue model is one of the best known and most widely used approaches for LCF analysis using plastic strain range. The characteristic life, N_f is dependent on the plastic strain range, $\Delta\varepsilon_p$, the fatigue ductility coefficient, C, and the fatigue exponent, m, given by the expression below

$$N_f^m \Delta\varepsilon_p = C$$

These constants were determined by Pang [24] for SnAgCu solder alloys which will be used in the Coffin-Manson model for this study. For temperature 125°C and frequency 0.001Hz, the constants m and C were taken as 0.853 and 9.2 respectively.

Schubert [22] proposed a fatigue model based on accumulated creep strain during one thermal cycle and characteristic life. The model was proposed for PBGA's, CSP's and Flip-Chip packages for both SnPbAg and SnAgCu solder alloys (see Figure 6.5). In this work we will examine the model for SAC solder. The equation for the model is given by

$$N_f = 4.5\ \varepsilon_{cr}^{(-1.295)}$$

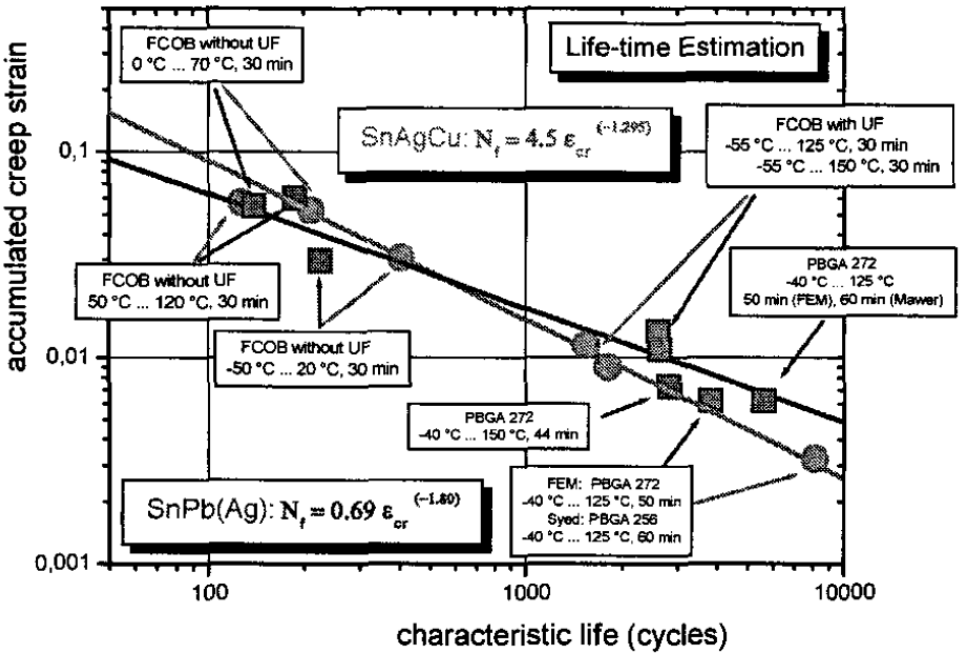

Figure 6.5 Schubert's strain based model for SAC and SnPb

6.2 Simulation

Three-dimensional non-linear finite element modeling was used to calculate the strain energy density accumulation (or plastic work) in solder joints. ANSYS v15.0 was leveraged for all aspects of analysis: pre-processing, solution and post-processing. Quarter symmetric model was considered to save computational time without compensating the accuracy of results.

The goal of the simulations was to calculate the plastic work per unit volume (or viscoplastic strain energy density) accumulated per thermal cycle for the critical solder which is most vulnerable to crack formation and failure. The critical solder joint for the QFN package is determined by plotting the contour of

equivalent (von-Mises) stress over the solder joints. The solder with the largest stress concentration is identified as the critical solder. Figure 6.6 shows the critical solder which is near to the package corner. This result is in line with experimental test result as shown in Figure 6.7. Pin 20 is the location near the package corner.

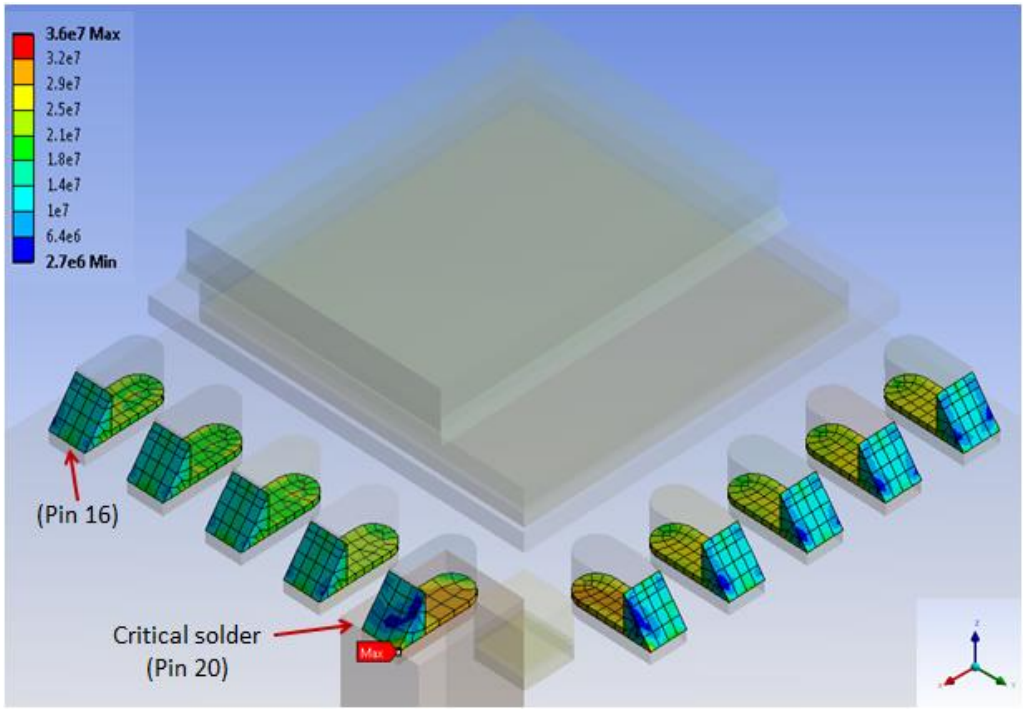

Figure 6.6 Equivalent stress (Pa) in solder joints (global model)

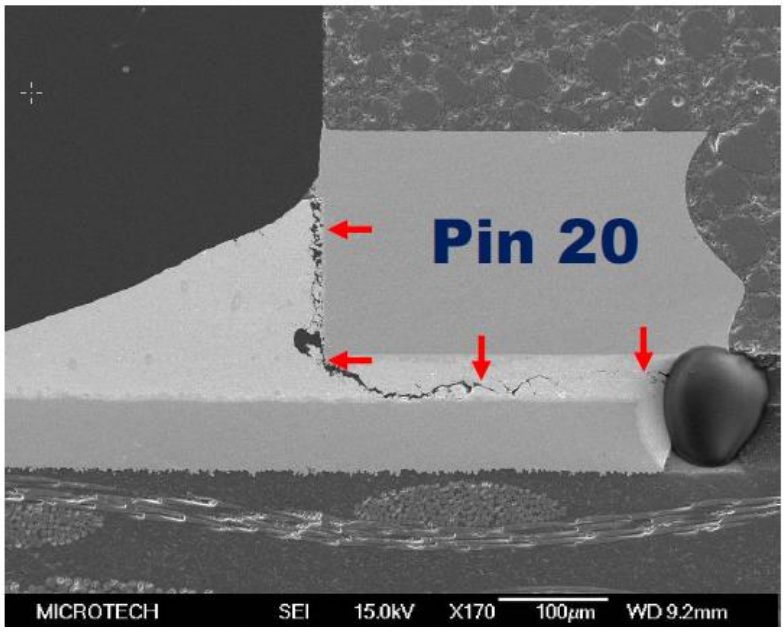

Figure 6.7 SEM image of critical solder joint

To obtain accurate results for the critical solder joint, sub model is designed for the critical solder with a unit cell as shown in Figure 5.8. The equivalent stress and strain energy on the critical solder obtained from the sub model is shown in Figure 6.8 and Figure 6.9. It can be clearly observed from Figure 6.8 that the maximum stress concentration occurs on the bottom layer of the solder and around the edge between the lead and the solder, which also correlates well with the SEM image showing the cracking failure.

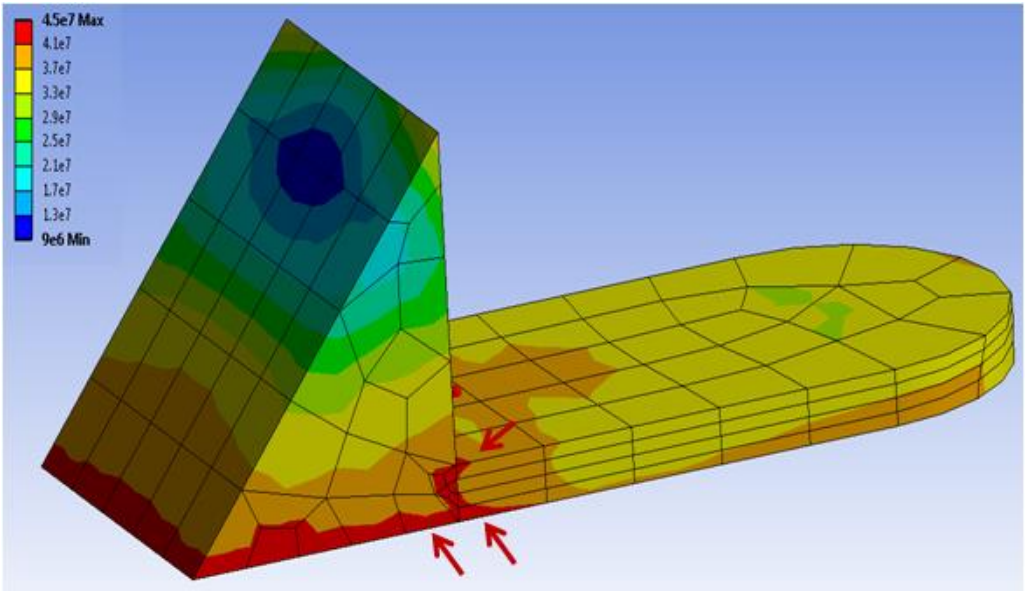

Figure 6.8 Equivalent stress (Pa) in the critical solder (sub model)

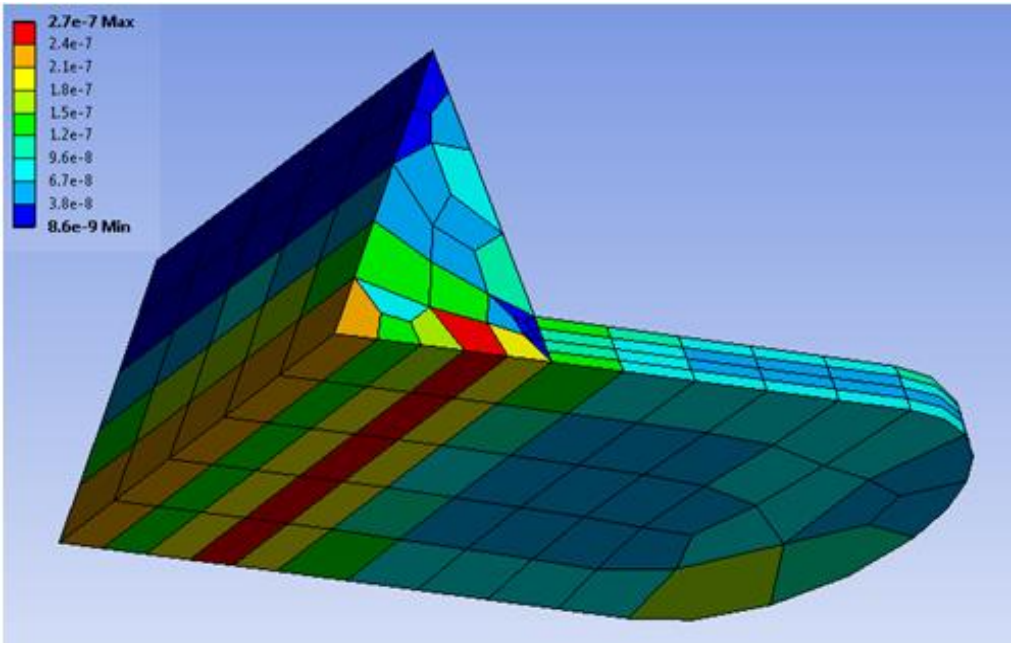

Figure 6.9 Strain energy (J) in critical solder (sub model)

The aim of the simulations is to calculate plastic work per unit volume (or viscoplastic strain energy density) by ANSYS at the end of second and third temperature cycles, which will be further used to predict the solder joint reliability using the fatigue models discussed in section 6.1. Three complete thermal cycles were simulated in this study to establish a stable stress-strain hysteresis loop. This choice is dependent on both computational time and stabilization of the system under thermal cycling [26]. As the element size in the solder joint decreases, the calculated strain energy density increases. Hence, volume averaging technique is leveraged to reduce this sensitivity to meshing. The strain energy value of each element is normalized by the volume of the element

$$\Delta W_{ave} = \frac{\Sigma\, \Delta \mathrm{W} \times \mathrm{V}}{\Sigma\, \mathrm{V}}$$

where ΔW_{ave} is the average viscoplastic strain energy density accumulated per cycle for the interface elements, ΔW is the viscoplastic strain energy density accumulated per cycle of each element, and V is the volume of each element. The summation runs through all elements in the selected set. The fatigue indicator is chosen to be the difference of ΔW_{ave} from the second and third temperature cycle.

$$\Delta W = (\Delta W_{ave})_{3rd} - (\Delta W_{ave})_{2nd}$$

Selection of the element set for volume averaging is very important since the fatigue results can vary significantly. In this work, four different approaches are used to select the element set to be processed for further analysis. Figure 6.10

shows the complete solder joint used as the element set and Figure 6.11 shows the different thickness layer used to extract the fatigue parameter.

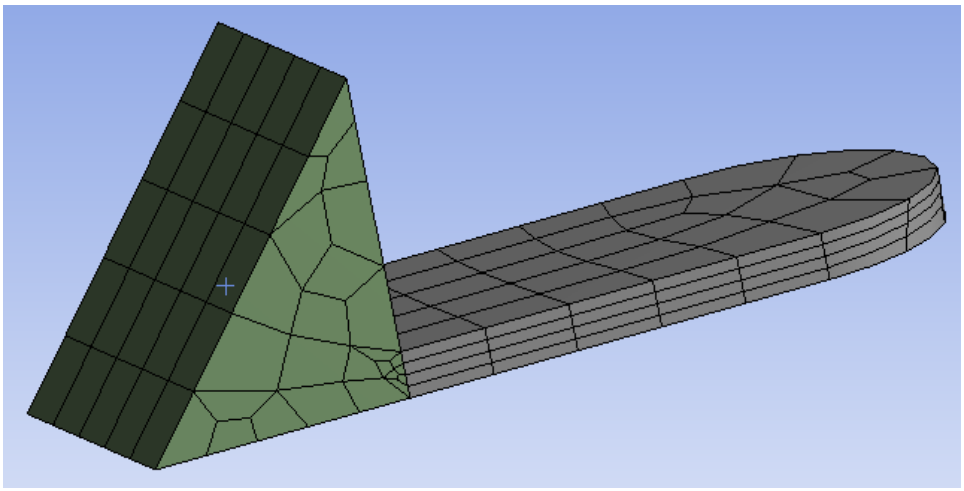

Figure 6.10 Complete solder joint used for volume averaging

Initially a 10μm thick layer from the bottom of the critical solder joint is selected for volume averaging. Subsequently, a 20μm and then a 30μm thick layer are selected. The average plastic work (strain energy density) for all the four cases is shown in Table 6.1.

Table 6.1 Element volume averaging results

Parameter	Complete solder	10μm thick bottom layer	20μm thick bottom layer	30μm thick bottom layer
ΔW (MPa)	0.96	1.72	1.49	1.58

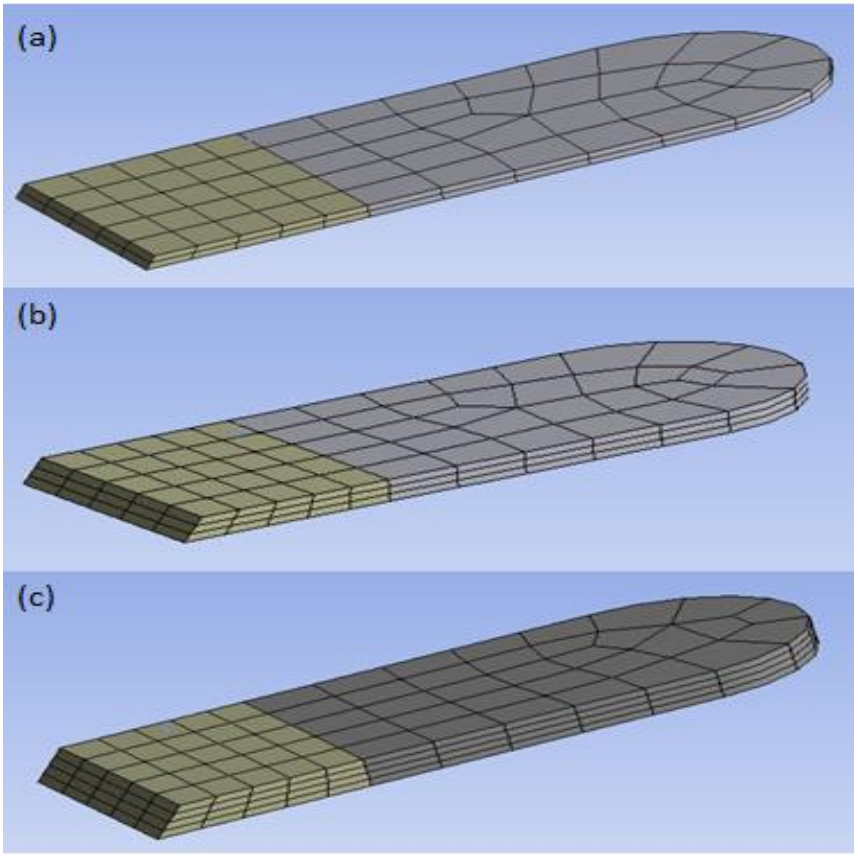

Figure 6.11 Different averaged layer (a) 10µm layer (b) 20µm layer (c) 30µm layer

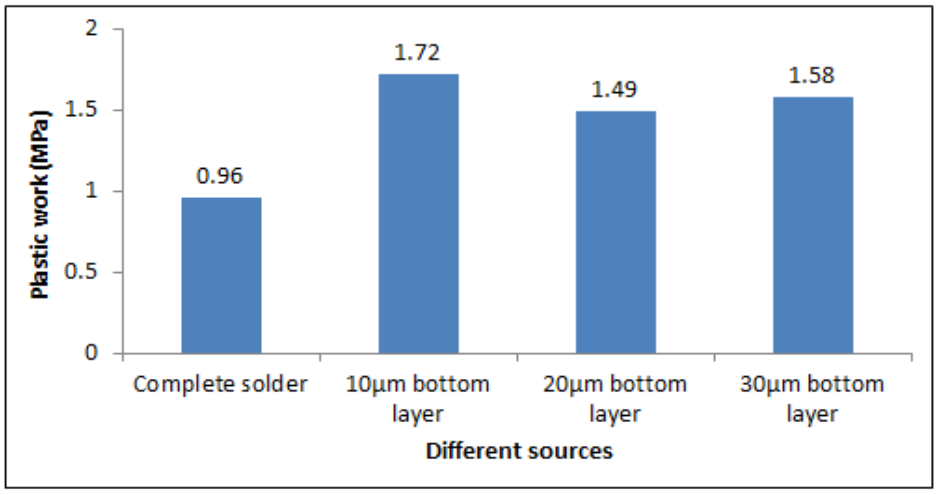

Figure 6.12 Plastic work comparison for different approaches

It can be clearly seen from Figure 6.12 that the plastic work fatigue parameter is sensitive to the location of the element selected for averaging. The whole solder averaged parameter will underestimate the plastic work and eventually overestimate the fatigue life accordingly since the element contains both maximum and minimum stress concentration zones. From Figure 6.8 it can be observed that the maximum stress concentration occurs at the bottom of the solder joint. As we keep on increasing the layer thickness for volume averaging, the plastic work decreases since we are moving away from the fatigue failure zone. The high plastic work for the 30µm layer over the 20µm layer can be explained due to the stress concentration on the top layer between the lead and solder (see Figure 6.8). Hence, the averaged parameter located on the bottom 10µm layer is appropriate for fatigue life prediction and this approach will be used for all analysis in this work. Figure 6.13 and Figure 6.14 shows the equivalent stress and strain energy distribution on the 10µm thick layer solder.

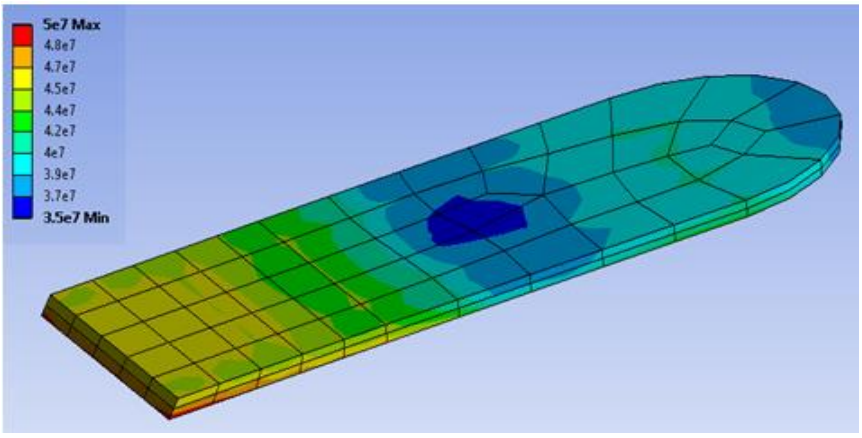

Figure 6.13 Equivalent stress (MPa) distribution on 10µm thick solder layer

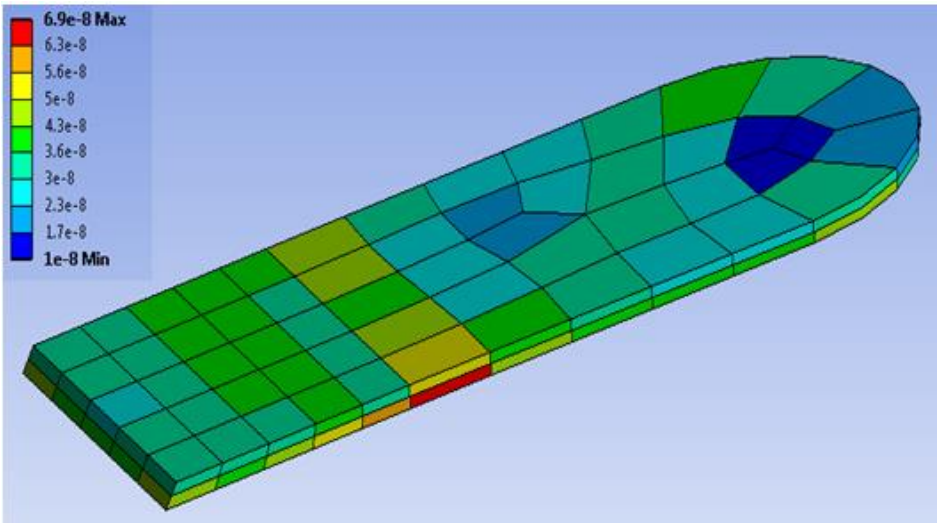

Figure 6.14 Strain energy (J) distribution on 10μm thick solder layer

Using the same methodology which was used to determine plastic work (strain energy density) using ANSYS, plastic strain range is also calculated by volume averaging over the 10μm thick solder layer.

$$\Delta\varepsilon_p = \left(\Delta\varepsilon_{pavg}\right)_{3rd} - \left(\Delta\varepsilon_{pavg}\right)_{2nd}$$

6.3 Fatigue Life Prediction Results

The plastic work and plastic strain-range are determined for QFN package under both thermal cycling conditions, TC1 and TC2 and then substituted into the fatigue models as discussed in section 6.1. The results obtained are then correlated to the experimentally measured characteristic lifetime (cycles to 63.2% failure) in the BLR tests as shown in Figure 6.15 and Figure 6.16. Table 6.2 through Table 6.7 shows the prediction results.

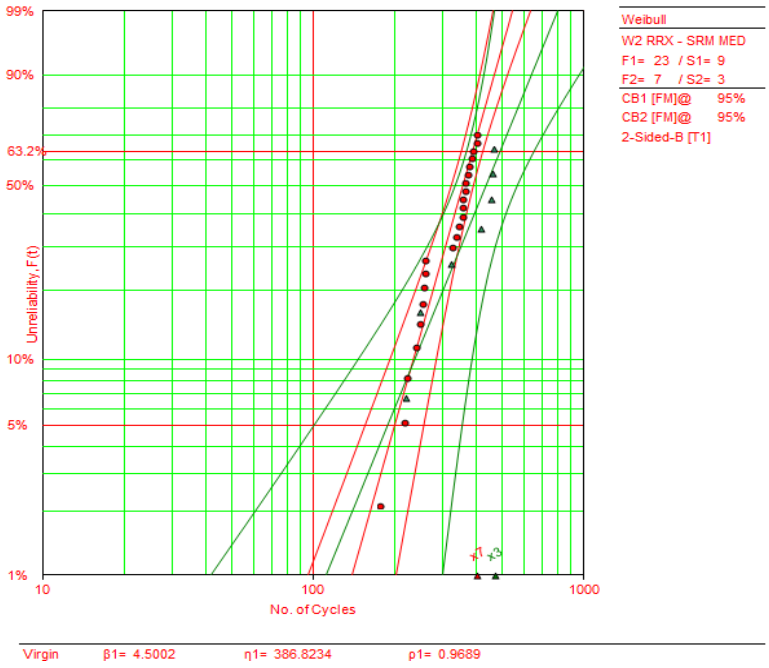

Figure 6.15 Weibull plot for QFN under TC1 thermal condition

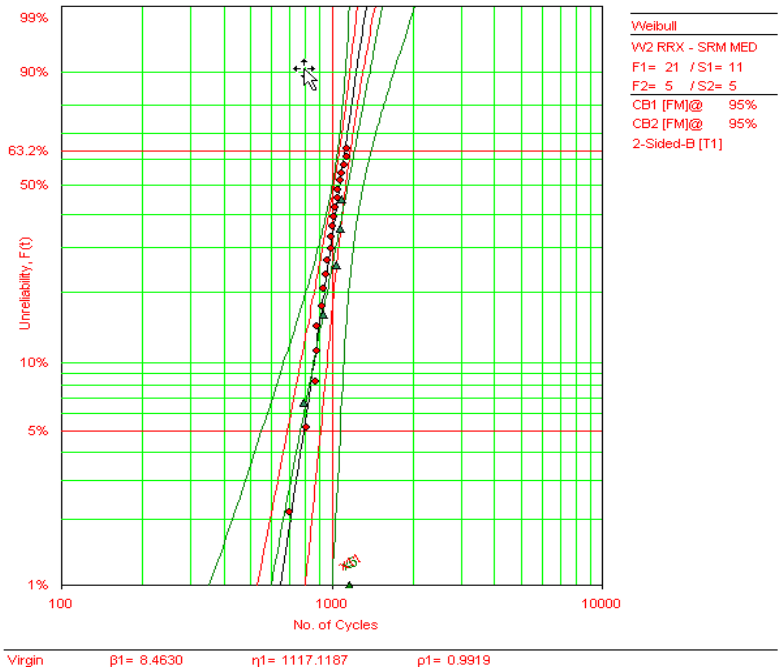

Figure 6.16 Weibull plot for QFN under TC2 thermal condition

Table 6.2 Comparison of lifetime predictions based on Wei Sun's model and BLR test

Condition	ΔW (MPa)	Calculated N_f (cycles)	BLR tests (cycles)	Error (%)
TC1	1.72	599.77	386.82	55.05
TC2	0.30	1184.44	1117.11	6.03

Table 6.3 Comparison of lifetime predictions based on Schubert's model and BLR test

Condition	ΔW (MPa)	Calculated N_f (cycles)	BLR tests (cycles)	Error (%)
TC1	1.72	198.24	386.82	-48.75
TC2	0.30	1174.14	1117.11	5.11

Table 6.4 Comparison of lifetime predictions based on Morrows's model and BLR test

Condition	ΔW (MPa)	Calculated N_f (cycles)	BLR tests (cycles)	Error (%)
TC1	1.72	327.49	386.82	-15.34
TC2	0.30	2285.21	1117.11	104.56

Table 6.5 Comparison of lifetime predictions based on Syed's model and BLR test

Condition	ΔW (MPa)	Calculated N_f (cycles)	BLR tests (cycles)	Error (%)
TC1	1.72	408.31	386.82	5.56
TC2	0.30	2041.63	1117.11	82.76

Table 6.6 Comparison of lifetime predictions based on Coffin Manson's model and BLR test

Condition	$\Delta\varepsilon_p$	Calculated N_f (cycles)	BLR tests (cycles)	Error (%)
TC1	0.05	470.66	386.82	21.67
TC2	0.01	2895.92	1117.11	159.23

Table 6.7 Comparison of lifetime predictions based on Schubert's model (plastic strain) and BLR test

Condition	$\Delta\varepsilon_p$	Calculated N_f (cycles)	BLR tests (cycles)	Error (%)
TC1	0.05	228.20	386.82	-41.01
TC2	0.01	1699.04	1117.11	52.09

From the results above it can be seen that a lot of discrepancies was observed between the predicted results and the BLR test. The relative error, which is defined as $(N_{calculated} - N_{test}) / N_{test}$ are larger than 41% except for few cases where the error is below 15%. These discrepancies are explained below for each specific model. Although Wei Sun's model was derived using QFN package, the solder material considered in the study was SAC405 using Schubert's constitutive model for Pb-free solder and having different material properties as compared to the one used in this study.

Schubert's study was done primarily on PBGA's and Flip Chip using SAC387 solder alloy. Substrates used in PBGA are plastic having low stiffness hence more flexible and warp more due to temperature changes during thermal cycling. This makes the solder joints in PBGA experience not only shear loading but also significant peel loading. Peel loading (mode I) is known to be more effective to advance cracks than shear loading (mode II) in fracture mechanics. Hence the low calculated fatigue life for TC1 for Schubert's model.

The constants for the Morrow's and Coffin-Manson model was derived using number of creep and fatigue tests on Pb-free solder alloy (SAC387).

Syed's model consisted of BGA and CSP packages using SnAgCu (4.0Ag0.5Cu or 3.9Ag0.5Cu) solder alloy.

From these facts, it can be concluded that the fatigue life prediction model is unique for a package family and the solder material used. Using a fatigue model

having met just one criterion will result in considerable error in life prediction as shown in the results above.

Hence a new fatigue model equation is needed to predict the characteristic life for QFN packages with SAC305 solder alloy. Based on the simulated fatigue correlation parameter (strain energy density and plastic strain range) and the corresponding experimental result, a new power equation is derived as shown in Figure 6.17 and Figure 6.18.

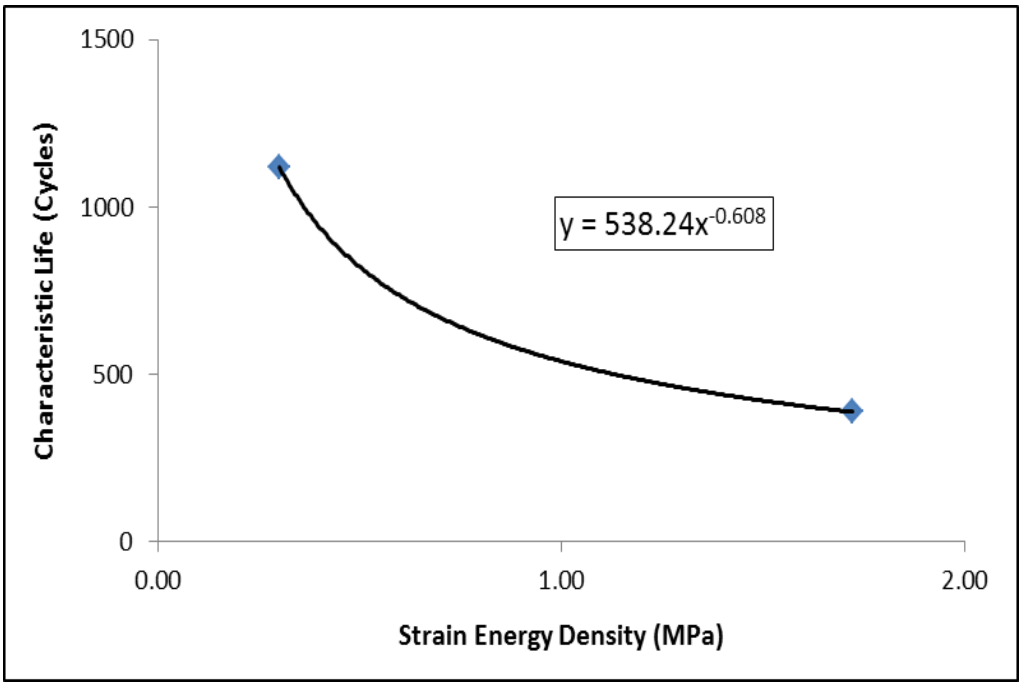

Figure 6.17 New strain energy density based model for QFN solder joint fatigue life prediction

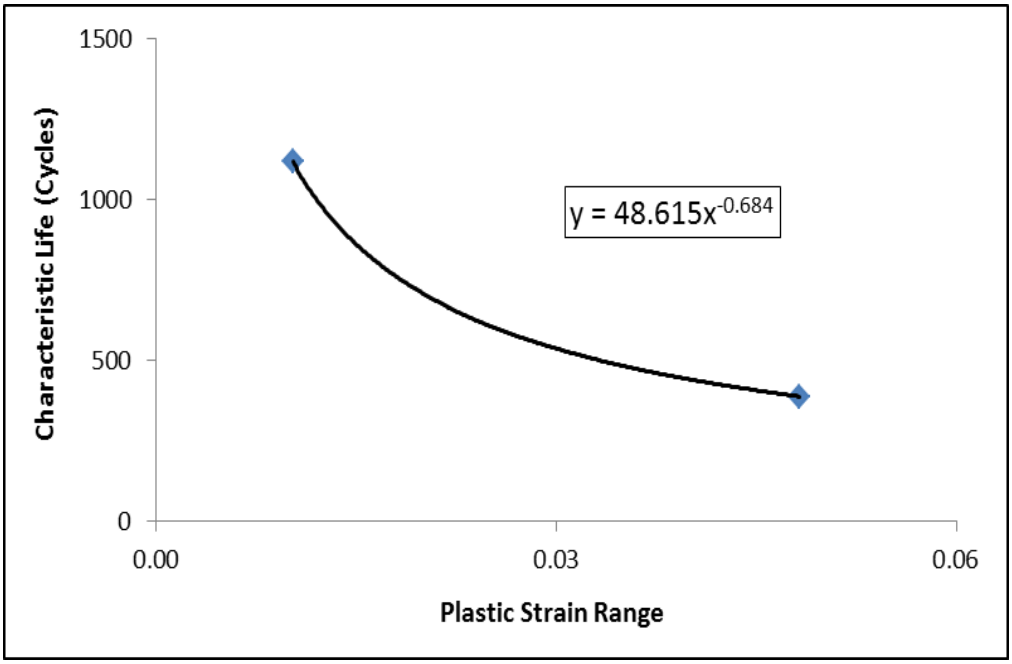

Figure 6.18 New plastic strain based model for QFN solder joint fatigue life prediction

Note that y in the graphs corresponds to N_f and x corresponds to ΔW_p and $\Delta\varepsilon_p$ depending on energy model and strain model respectively. Since only two BLR test data were available to plot these equations, there is a high probability that the predicted results using these equation would give highly inaccurate values. Once additional experimental thermal cycling tests are done on these QFN packages, using the new data points an accurate power equation can be derived using the same methodology. These equations are unique for this QFN package family and SAC305 solder joint.

Chapter 7

DESIGN ANALYSIS OF QFN

In this design study the effects of some of the key package parameters such as package geometry and material properties is investigated in an attempt to improve the solder joint reliability of the QFN. The parameters in focus are Die size, CTE of Mold compound, Solder stand-off height and CTE of PCB. Only one package parameter is modified at a time to study its effect on the solder joint reliability. The analysis is done on QFN package with the same material properties but on 134mil thick board.

The main objective is to study the effects on these key parameters on the solder joint fatigue life to support package design for reliability in different applications.

7.1 Effect of Die Size

Selecting smaller die size is better for reliability because the die edge is farther from the peripheral solder joint thus resulting in less local CTE mismatch. Reducing the die size by 30% i.e. from 4.315 x 3.245 mm to 3.02 x 2.27 gives an 8% better reliability.

Table 7.1 Effect of die size

Parameter	Design values (mm)	ΔWp (MPa)	% difference
Die size	4.315 x 3.245	2.01	-
	3.02 x 2.27	1.86	-8

7.2 Effect of Mold CTE

The material selection of mold compound plays a crucial role in the solder joint reliability of the package. The Coefficient of thermal expansion (CTE) of mold used in this study is 63ppm/°C which is quite high. Due to this high difference in CTE between the mold and the package components (die pad and exposed pad); thermal stresses are induced resulting in warpage which has a direct result on the solder joint. By using an optimum material for mold compound, the reliability can be improved by 76%.

Table 7.2 Effect of Mold CTE

Parameter	Design values (ppm/°C)	ΔWp (MPa)	Percentage difference
Mold CTE	63	2.01	-
	50	1.23	-39
	40	0.92	-55
	17	0.48	-76

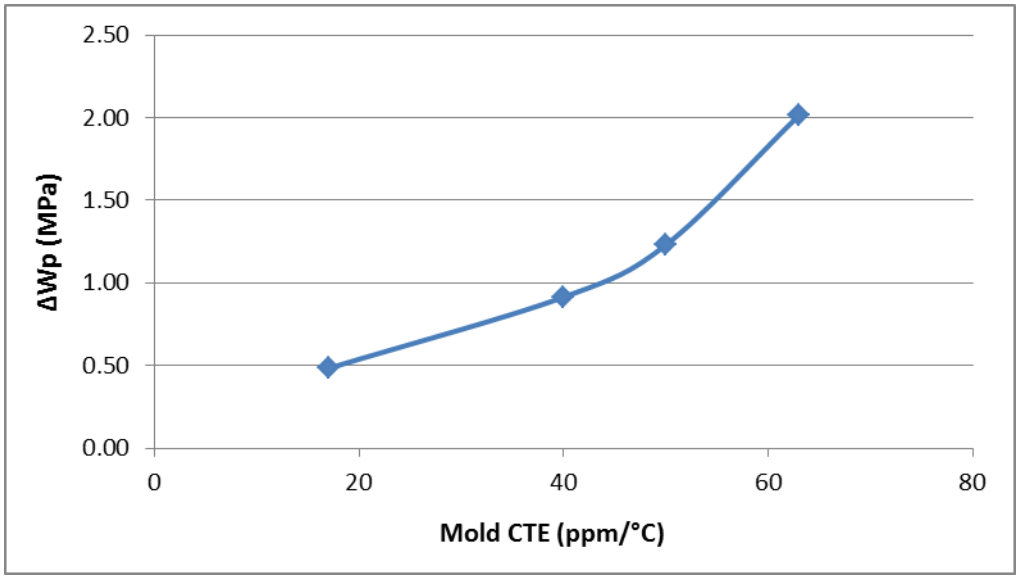

Figure 7.1 Graph of SED vs CTE of mold

7.3 Effect of Solder Stand-off height

Generally, higher solder stand-off height has longer fatigue life. The larger solder thickness helps to reduce the SED induced during thermal cycling. Also more solder volume means more resistance to the crack propogation in the solder joint. By increasing the height from 30µm to 50µm, the reliability increases by 23%.

Note the element selection for volume averaging in this case was not done on the 10µm thick layer but instead on the whole 30µm thick layer to have a direct comparison on increase in the solder thickness on the solder joint reliability.

Table 7.3 Effect of solder stand-off height

Parameter	Design values (μm)	ΔWp (MPa)	Percentage difference
Stand-off height	30	1.57	-
	50	1.21	-23

7.4 Effect of PCB CTE

The CTE of PCB plays an important role in the warpage of the package. With a change in CTE of PCB by 4ppm/°C in both in plane and out of plane, about 9% increase in reliability is achieved.

Table 7.4 Effect on PCB CTE

Parameter	Design values (ppm/°C)	ΔWp (MPa)	Percentage difference
PCB CTE	α_{xy}= 16, α_z= 84	2.01	-
	α_{xy}= 12, α_z= 80	1.83	-9

From Figure 7.2 it can be seen that Mold compound has a high effect of 76% whereas other parameters have either considerable or little effect of 23% to 8% on solder joint reliability.

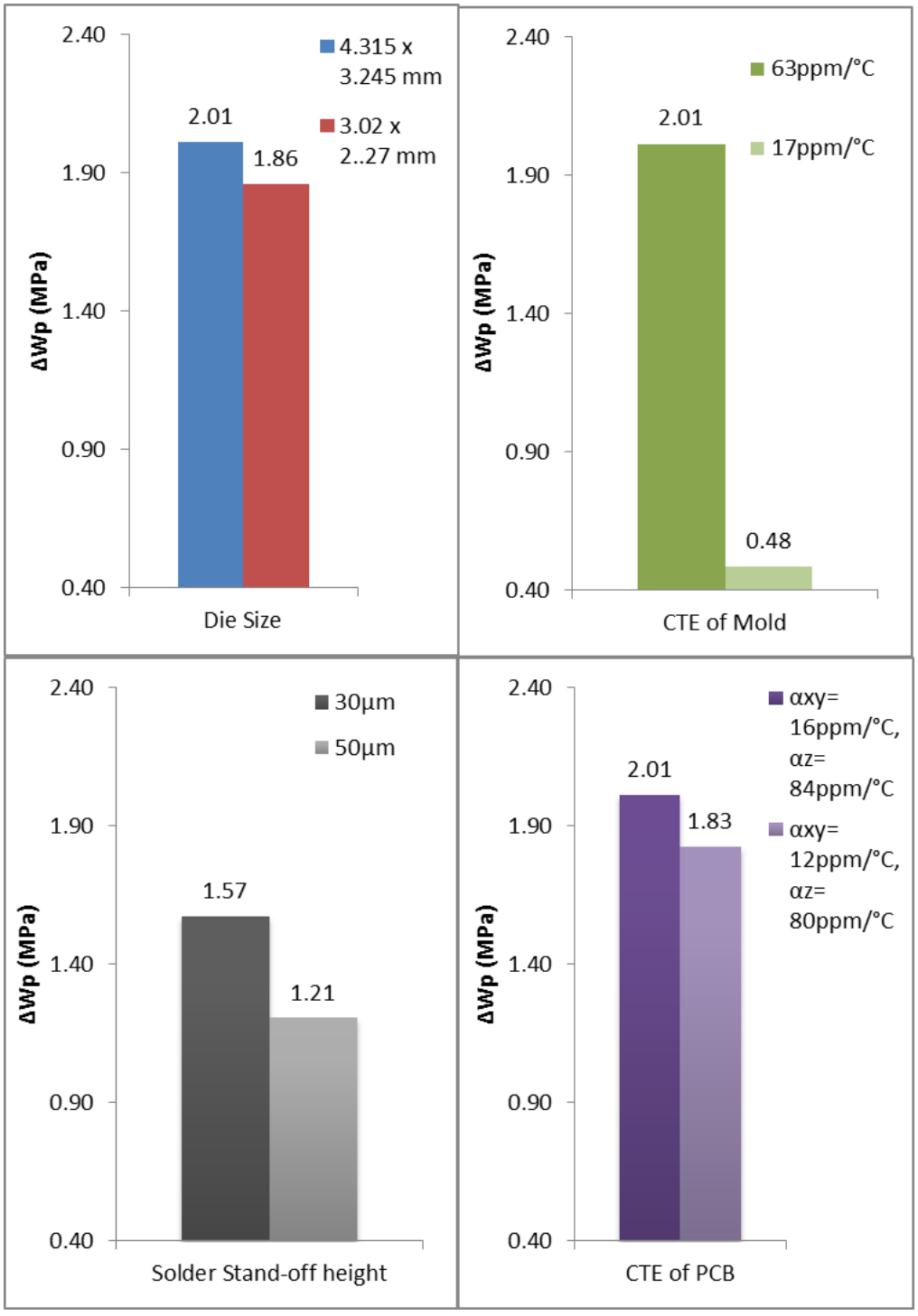

Figure 7.2 Comparison of various package parameters on reliability

Another interesting thing to note is the effect of increase in the PCB thickness on the solder joint reliability of the package. Table 7.5 shows the plastic work for the both the cases.

Table 7.5 Effect of PCB thickness

Parameter	Design values (mil)	ΔWp (MPa)	% difference
PCB thickness	93	1.72	-
	134	2.01	17

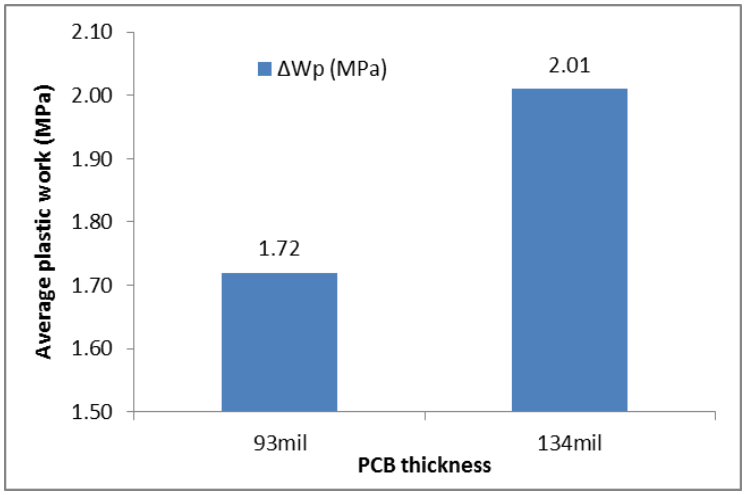

Figure 7.3 Comparison of PCB thickness on reliability

It's clear from the Figure 7.3 that as the PCB thickness increases, the reliability of the solder joint decreases. For this case, the 134mil has 17% more fatigue damage as compared to the 93mil board. This is because thicker boards are stiffer and less flexible during warping under thermal cycling hence transfer more stress onto the solder joints resulting in early failures.

Chapter 8

CONCLUSION

8.1 Summary and Conclusion

A 3D Finite Element model for QFN package was analyzed in this study to assess the board level reliability under thermal cycling. Design for reliability method was used to approach this problem. The study was divided in three sections. First section involved simulation of the FE model using ANSYS to deduce the fatigue correlation parameter (average plastic work and plastic strain range). Anand's viscoplastic constitutive law was used to describe the inelastic behavior of the lead-free solder (SAC305). The test vehicle was a 6x6mm QFN package on a 93mil FR-4 board subjected under two thermal cycling conditions, TC1 and TC2. It was demonstrated that the 10μm thick layer of solder from the critical solder joint was the appropriate method for volume averaging to determine the fatigue life. The fatigue correlation parameter deduced from the simulation is then used to examine various energy based models and strain based models. It is found that the fatigue life prediction models are unique for a package family and the solder material used.

The second section addressed the need for a new fatigue model for the QFN package. Based on the simulated fatigue correlation parameter and the corresponding BLR experimental result, a new power equation was derived which is unique for this QFN package and SAC305 solder alloy.

In the third section, design analysis was performed on QFN package with 134mil FR-4 board with an attempt to improve the solder joint reliability. It was concluded that for better reliability it is recommended to have smaller die size, lower CTE of mold compound and PCB, larger solder stand-off height and thinner board.

Fatigue modeling can be applied for design analysis of board level reliability to save cost, time, and manpower in performing the Design of Experiment (DOE) studies by thermal cycling simulations. This analysis is especially useful for new package development. The fatigue modeling can also be integrated with electrical simulation and thermal analysis for a complete board-level reliability design solution.

8.2 Future Work

The aim of this study was to develop a new energy and strain based fatigue model to accurately predict the characteristic life of the solder joint. In this work only two BLR test results were available. Once more tests are performed on the QFN package; using these results an accurate power equation can be derived.

Also, a comprehensive design analysis of QFN can be performed on all the key parameters and design optimization can be executed to check which set of parameters when used together gives highest reliability for the solder joint. A multi-variable design optimization can be executed for the same.

APPENDIX A

APDL SCRIPT FOR PLASTIC WORK

```
!APDL SCRIPT TO CALCULATE PLASTIC WORK

/post1
allsel,all
!CALC AVG PLASTIC WORK FOR CYCLE1

set,5,last,1                    !LOAD STEP
cmsel,s,botsolder,elem          !ELEMENT FOR VOL AVERGAING

etable,vo1table,volu
pretab,vo1table
etable,vse1table,nl,plwk        !PLASTIC WORK
pretab,vse1table

smult,pw1table,vo1table,vse1table

ssum
*get,splwk,ssum,,item,pw1table
*get,svolu,ssum,,item,vo1table

pw1=splwk/svolu                 !AVERAGE PLASTIC WORK

!CALC AVG PLASTIC WORK FOR CYCLE2

set,10,last,1                   !LOAD STEP
cmsel,s,botsolder,elem

etable,vo2table,volu
pretab,vo2table
etable,vse2table,nl,plwk        !PLASTIC WORK
pretab,vse2table

smult,pw2table,vo2table,vse2table

ssum
*get,splwk,ssum,,item,pw2table
```

```
*get,svolu,ssum,,item,vo2table

pw2=splwk/svolu                 !AVERAGE PLASTIC WORK


!CALC DELTA AVG PLASTIC WORK
pwa=pw2-pw1

!CALC AVG PLASTIC WORK FOR CYCLE3

set,15,last,1                   !LOAD STEP
cmsel,s,botsolder,elem

etable,vo3table,volu
pretab,vo3table
etable,vse3table,nl,plwk        !PLASTIC WORK
pretab,vse3table

smult,pw3table,vo3table,vse3table

ssum
*get,splwk,ssum,,item,pw3table
*get,svolu,ssum,,item,vo3table

pw3=splwk/svolu                 !AVERAGE PLASTIC WORK


!CALC DELTA AVG PLASTIC WORK

pwb=pw3-pw2
```

APPENDIX B

APDL SCRIPT FOR PLASTIC STRAIN

```
!APDL SCRIPT TO CALCULATE PLASTIC STRAIN

/post1
allsel,all
!CALC AVG PLASTIC STRAIN FOR CYCLE1

set,5,last,1                    !LOAD STEP
cmsel,s,botsolder,elem          !ELEMENT FOR VOL AVERGAING

etable,vo1table,volu
pretab,vo1table
etable,vse1table,nl,epeq        !PLASTIC STRAIN
pretab,vse1table

smult,ps1table,vo1table,vse1table

ssum
*get,sepeq,ssum,,item,ps1table
*get,svolu,ssum,,item,vo1table

epeqavg1=sepeq/svolu            !AVERAGE PLASTIC STRAIN


!CALC AVG PLASTIC STRAIN FOR CYCLE2

set,10,last,1                   !LOAD STEP
cmsel,s,botsolder,elem          !ELEMENT FOR VOL AVERGAING

etable,vo3table,volu
pretab,vo3table
etable,vse3table,nl,epeq        !PLASTIC STRAIN
pretab,vse3table

smult,ps2table,vo3table,vse3table

ssum
```

```
*get,sepeq,ssum,,item,ps2table
*get,svolu,ssum,,item,vo3table

epeqavg2=sepeq/svolu                !AVERAGE PLASTIC STRAIN

! CALC DELTA AVG PLASTIC STRAIN

epeqavga=epeqavg2-epeqavg1


!CALC AVG PLASTIC STRAIN FOR CYCLE3

set,15,last,1                       !LOAD STEP
cmsel,s,botsolder,elem              !ELEMENT FOR VOL AVERGAING

etable,vo5table,volu
pretab,vo5table
etable,vse5table,nl,epeq            !PLASTIC STRAIN
pretab,vse5table

smult,ps3table,vo5table,vse5table

ssum
*get,sepeq,ssum,,item,ps3table
*get,svolu,ssum,,item,vo5table

epeqavg3=sepeq/svolu                !AVERAGE PLASTIC STRAIN


! CALC DELTA AVG PLASTIC STRAIN

epeqavgb=epeqavg3-epeqavg2
```

REFERENCES

[1] G. Q. Zhang, *Mechanics of Microelectronics*, XIV ed. Springer, 2006.

[2] Y. B. Quek, "QFN Layout Guidelines," Texas Instruments, 2006.

[3] R. Rodgers, "Cypress Board Level Reliability Test for Surface Mount Packages," Cypress Seminconductor White paper, 2012.

[4] T. Y. Tee, H. S. Ng, D. Yap, and Z. Zhong, "Comprehensive board-level solder joint reliability modeling and testing of QFN and PowerQFN packages," in *ECTC*, Singapore, 2002, pp. 985-991.

[5] A. Syed, "BOARD LEVEL ASSEMBLY AND RELIABILITY CONSIDERATIONS FOR QFN TYPE PACKAGES," Amkor.

[6] C. Birzer and S. Stoeckl, "Reliability investigations of leadless QFN packages until end-of-life with application-specific board-level stress tests," in *ECTC*, San Diego, 2006.

[7] L. Li, "Reliability modeling and testing of advanced QFN packages," in *ECTC*, Las Vegas, 2013.

[8] J. Vries and M. Jansen, "Solder-joint reliability of HVQFN-packages subjected to thermal cycling," *Microelectronics Reliability*, vol. 49, no. 3, p. 331–339, Mar. 2009.

[9] W. Sun, W. H. Zhu, and R. Danny, "Study on the Board-level SMT

Assembly and Solder Joint Reliability of Different QFN Packages," in *EuroSimE IEEE*, London, 2007, pp. 1-6.

[10] S. Stoeckl, "Improving the solder joint reliability of VQFN packages," in *EPTC*, Singapore, 2005.

[11] "IPC-9592, Performance Parameters for Power Conversion Devices," Standard.

[12] J. N. Reddy, *An Introduction to the Finite Element Method*, 3rd ed. McGraw-Hill, 2005.

[13] T. Raman, "Assessment of The Mechanical Integrity of CU/LOW-K Dielectric In A Flip Chip Package," Master's Thesis, UT Arlington, Arlington, 2012.

[14] E. Madenci, *The Finite Element Method and Applications in Engineering Using ANSYS*, XVI ed. Springer, 2007.

[15] "Introduction to ANSYS Meshing" Lecture 3, 15.0 Release.

[16] (2014) ANSYS Documentation. [Online]. http://www.ansys.com

[17] J. Pang, *Lead Free Solder: Mechanics and Reliability*, X ed. Springer, 2012.

[18] J. Zhao, V. Gupta, A. Lohia, and D. Edwards, "Reliability Modeling of Lead-Free Solder Joints in Wafer-Level Chip Scale Packages," *Journal of Electronic Packaging*, vol. 132, no. 1, p. 6, Mar. 2010.

[19] R. Darveaux, "Effect of simulation methodology on solder joint crack growth correlation," in *ECTC*, Las Vegas, 2000.

[20] L. F. Coffin, "A study of the effects of cyclic thermal stresses on a ductile metal," ASME, 1954.

[21] S. S. Manson, "Fatigue: a complex subject-some simple approximation," Exp Mech 5(7):193–226, 1965.

[22] A. Schubert, R. Dudek, and E. Auerswald, "Fatigue life models for SnAgCu and SnPb solder joints evaluated by experiments and simulation," in *ECTC*, New Orleans, 2003, pp. 603-610.

[23] J. D. Morrow, "Cyclic plastic strain energy and fatigue of metals," American Society for Testing and Materials Testing Standard ASTM STP 378, 1964.

[24] J. H. Pang, B. S. Xiong, and T. H. Low, "Creep and fatigue characterization of lead free 95.5Sn-3.8Ag-0.7Cu solder," in *ECTC*, 2004, pp. 1333-1337Vol2.

[25] A. Syed, "Accumulated creep strain and energy density based thermal fatigue life prediction models for SnAgCu solder joints," in *ECTC*, 2004, pp. 737-746Vol1.

[26] X. Fan, M. Pei, and P. K. Bhatti, "Effect of finite element modeling techniques on solder joint fatigue life prediction of flip-chip BGA packages,"

in *ECTC*, San Diego, 2006.

BIOGRAPHICAL STATEMENT

Tejas Shetty received his Bachelor's degree in Mechanical Engineering from the University of Mumbai in the year 2010. He then decided to work for FLSmidth Pfister India Limited, Mumbai as a Design Engineer for 2 years, from 2010 to 2012. He decided to pursue his Master's in Mechanical Engineering by enrolling in University of Texas at Arlington in Fall 12. There he joined the Electronics MEMS & Nanoelectronics Systems Packaging Center (EMNSPC) under Dr. Dereje Agonafer and developed a keen interest in reliability and failure analysis of electronic packages. His research interest includes reliability, fracture mechanics, thermo-mechanical simulation and material characterization. During his time, he was an integral part of the SRC funded project where he worked closely with the industry liaisons. Upon graduation, Tejas plans to pursue his career in the semiconductor industries.